Itinerary synchronization between PWL systems coupled with unidirectional links

A. Anzo-Hernández[a], E. Campos-Cantón[b*] and Matthew Nicol[c]

[a]Cátedras CONACYT - Benemérita Universidad Autónoma de Puebla,
Facultad de Ciencias Físico-Matemáticas,
Benemérita Universidad Autónoma de Puebla,
Avenida San Claudio y 18 Sur, Colonia San Manuel, 72570.
Puebla, Puebla, México. *andres.anzo@hotmail.com*

[b]División de Matemáticas Aplicadas,
Instituto Potosino de Investigación Científica y Tecnológica A.C.
Camino a la Presa San José 2055 col. Lomas 4a Sección, 78216, San Luis Potosí, SLP, México. *eric.campos@ipicyt.edu.mx,** Corresponding author.

[c]Mathematics Department, University of Houston,
Houston, Texas,
77204-3008, USA. *nicol@math.uh.edu.*

Abstract

In this paper the collective dynamics of N-coupled piecewise linear (PWL) systems with different number of scrolls is studied. The coupling is in a master-slave sequence configuration, with this type of coupling we investigate the synchrony behavior of a ring-connected network and a chain-connected network both with unidirectional links. Itinerary synchronization is used to detect synchrony behavior. Itinerary synchronization is defined in terms of the symbolic dynamics arising by assigning different numbers to the regions where the scrolls are generated. A weaker variant of this notion, ϵ-itinerary synchronization is also introduced and numerically investigated. It is shown that in certain parameter regimes if the inner connection between nodes takes account of all the state variables of the system (by which we mean that the inner coupling matrix is the identity matrix), then itinerary synchronization occurs and the coordinate motion is determined by the node with the smallest number of scrolls. Thus the collective behavior in all the nodes of the network is determined by the node with least scrolls in its attractor. Results about the dynamics in a directed chain topology are also presented. Depending on the inner connection properties, the nodes present multistability or preservation of the number of scrolls of the attractors.

keywords: Itinerary Synchronization; chaos; dynamical networks; multiscroll attractor.

1 Introduction

Piecewise linear (PWL) systems are used to construct simple chaotic oscillators capable of generating various multiscroll attractors in the phase space. These systems contain a linear part plus a nonlinear element characterized by a switching law. One of the most studied PWL system is the so called Chua's circuit, whose nonlinear part (also named the Chua diode) generates two scroll attractors [1, 2]. Inspired by the Chua circuit, a great number of PWL systems have been produced via various switching systems [3]. A review and summary of different approaches to generate multiscroll attractors can be found in [4, 5, 6] and references therein.

Synchronization phenomena in a pair of coupled PWL systems has also attracted attention in the context of nonlinear dynamical systems theory and its applications [7, 8].

In general, we say that a set of dynamical systems achieve synchronization if trajectories in each system approach a common trajectory (in some sense) by means of interactions [9].

One way to study synchronization in a pair of PWL systems is to couple them in a master-slave configuration [1, 10]. In [11] the dynamical mechanism leading to projective synchronization of Chua circuits with different scrolls is investigated. In [12], a master-slave system composed of PWL systems is considered in which the slave system displays more scrolls in its attractor than the master system. The main result is that the slave system synchronizes with the master system by reducing its number of attractor scrolls, while the master preserves its number of scrolls. A consequence is the emergence of multistability phenomena. For instance, if the number of scrolls presented by the master system is less than the number of scrolls presented by the slave system, then the slave system can oscillate in multiple basins of attraction depending on its initial condition. Conversely, when the system of [12] is adjusted so that the master system displays more scrolls than the slave system when uncoupled then the slave system increases its number of attractor scrolls to equal that of the master system when coupled.

We study a system composed of an ensemble of master-slave systems coupled in a ring configuration network; *i.e.*, a dynamical network where each node is a PWL-system with varying numbers of scrolls in the attractors and connected in a ring topology with directional links. In order to address this problem, we introduce three concepts: 1) scroll-degree, which is defined as the number of scrolls of an attractor in a given node; 2) a network of nearly identical nodes, *i.e.*, a dynamical network composed of PWL systems with perhaps different scroll degree but similar underlying differential equations and 3) itinerary synchronization based on symbolic dynamics. A PWL system is defined by means of a partition of the space where linear systems act, so this natural partition is useful for analyzing synchronization between dynamical systems by using symbolic dynamics. Of course itinerary synchronization does not imply complete synchronization, where trajectories converge to a single one. In this paper we study the emergence of itinerary synchronization, ϵ-itinerary synchronization,

multistability and the preservation of the scroll number of a network of nearly identical nodes. Furthermore, we remove a link to the ring topology in order to study the effect of topology changes in the collective dynamics of the network. That is, we modify the topology by deleting a single link, transforming the structure to a directed chain of coupled systems which we call an open ring. We have formulated two possible scenarios after the link deletion: a) the first node in the chain has the largest scroll-degree or, b) it has the smallest one. In both scenarios we assume that the inner coupling matrix is the identity matrix *i.e.* the coupling between any pair of nodes is throughout all its state variables.

To the best of our knowledge, multistability and scroll-degree preservation have not been studied in the context of PWL dynamical networks. We note that Zhao *et.al.* in [14] established synchronization criteria for certain networks of non-identical nodes with the same equilibria point [14]. The authors proposed stability conditions in terms of inequalities involving matrix spectra which are, computationally speaking, difficult to solve. Sun *et.al.* in [13] studied the case in which nodes are nearly identical in the sense that each node has a slight parametric mismatch. The authors proposed an extension of the master stability functions for these types of dynamical network.

We have organized this paper as follows: In section 2 we introduce some mathematical preliminaries. In section 3 we give an easy approach to generate a one dimensional grid multiscroll attractor via PWL systems. In section 4 we introduce a partition to configure the symbolic dynamics of trajectories of a pair of coupled PWL systems. In section 5 we propose a definition of itinerary synchronization based on the itinerary of trajectories of a master-slave system. In section 6 we give some preliminaries of dynamical networks which are composed of N coupled dynamical systems. In section 7 the dynamics of N-coupled PWL systems in a ring topology network is analyzed. Some examples about itinerary synchronization are studied and different forms of couplings are also considered. Finally, in section 8 we discuss conclusions.

2 Mathematical Preliminaries

2.1 Piecewise linear dynamical systems

Let $T : X \to X$, with $X \subset \mathbb{R}^n$ and $n \in \mathbb{Z}^+$, be a piecewise linear dynamical system whose dynamics is given by a family of sub-systems of the form

$$\dot{\mathcal{X}} = A_\tau \mathcal{X} + B_\tau, \tag{1}$$

where $\mathcal{X} = (x_1, \ldots, x_n)^T \in \mathbb{R}^n$ is the state vector, $A_\tau = \{\alpha_{ij}^\tau\} \in \mathbb{R}^{n\times n}$, with $\alpha_{ij}^\tau \in \mathbb{R}^+$, and $B_\tau = (\beta_{\tau 1}, \ldots, \beta_{\tau n})^T \in \mathbb{R}^n$ are the linear operators and constant real vectors of the τth-subsystems, respectively. The index $\tau \in \mathcal{I} = \{1, \ldots, \eta\}$ is given by a rule that switches the activation of a sub-system in order to determine the dynamics of the PWL system. Let X be a subset of $\mathbb{R}^n$ and $\mathcal{P} = \{P_1, \ldots, P_\eta\}$ ($\eta > 1$) be a finite partition of X, that is, $X = \bigcup_{1\leq i\leq \eta} P_i$, and $P_i \cap P_j = \emptyset$ for $i \neq j$. Each element of the set $\mathcal{P}$ is called an atom.

The selection of the index τ can be given according to a predefined itinerary and controlling by time; or by requiring that τ takes its value according to the state variable χ depending upon which atom of a finite partition of the state-space $\mathcal{P} = \{P_1, \ldots, P_\eta\}$ ($\eta \in \mathbb{Z}^+$) a point is in.

An easy way to generate a partition $\mathcal{P}$ is to consider a vector $\mathbf{v} \in \mathbb{R}^n$ (with $\mathbf{v} \neq 0$) and a set of scalars $\delta_1 < \delta_2 < \cdots < \delta_{\eta-1}$ such that each $P_i = \{\mathcal{X} \in \mathbb{R}^n : \delta_{i-1} \leq \mathbf{v}^T\mathcal{X} < \delta_i\}$, with $i = 2, \ldots, \eta-1$, $P_1 = \{\mathcal{X} \in \mathbb{R}^n : \mathbf{v}^T\mathcal{X} < \delta_1\}$, and $P_\eta = \{\mathcal{X} \in \mathbb{R}^n : \delta_{\eta-1} \leq \mathbf{v}^T\mathcal{X}\}$. We call the hyperplanes $\mathbf{v}^T\mathcal{X} = \delta_i$ ($i = 1, \ldots, \eta-1$) the switching surfaces. Without loss of generality, we assume that the hyperplanes $\mathbf{v}^T\mathcal{X} = \delta_i$ (for $i = 1, 2, \ldots, \eta-1$) are defined with $\mathbf{v} = (1, 0, \ldots, 0)^T \in \mathbb{R}^n$.

In this paper we consider a piecewise linear system $(T, \mathcal{P})$, such that its restriction to each atom P_i has a fixed point $\mathcal{X}_i^*$ i.e. $T(\mathcal{X}_i^*) = 0$ for one $\mathcal{X}_i^* \in P_i$ ($i \in \mathcal{I}$). Clearly $\mathcal{X}_i^* = -A_\tau^{-1}B_\tau$. We assume that the switching signal depends on the state variable and is defined as follows:

Definition 2.1. Let $\mathcal{I} = \{1, 2, \ldots, \eta\}$ be an index set that labels each element of the family of the sub-systems (1). A function $\kappa : \mathbb{R}^n \to \mathcal{I} = \{1, \ldots, \eta\}$ of the form

$$\kappa(\mathcal{X}) = \begin{cases} 1, & \text{if} \quad \mathcal{X} \in P_1; \\ 2, & \text{if} \quad \mathcal{X} \in P_2; \\ \vdots & \quad\quad \vdots \\ \eta, & \text{if} \quad \mathcal{X} \in P_\eta; \end{cases} \tag{2}$$

is called a switching signal. Furthermore, if $\kappa(\mathcal{X}) = \tau_i \in \mathcal{I}$ is the value of the switching signal during the time interval $t \in [t_i, t_{i+1})$, then $\mathcal{S}(\mathcal{X}_0) = \{\tau_0, \tau_1, \ldots, \tau_m, \ldots\}$ gives the itinerary generated by $\kappa(\mathcal{X}_0)$ at $\mathcal{X}_0$ and, $\mathcal{S}(i, \mathcal{X}_0)$ is the element $\tau_i \in \mathcal{S}(\mathcal{X}_0)$ that occurs at time t_i, this defines a set of switching times $\Delta_t = \{t_0, t_1, \ldots, t_m, \ldots\}$.

Note that τ changes only when the orbit $\phi(t, \chi_0)$ goes from one atom P_i to another P_j, $i \neq j$.

Definition 2.2. A η-PWL system is composed of two sets: $\mathbf{A} = \{A_1, \ldots, A_\eta\}$ and $\mathbf{B} = \{B_1, B_2, \ldots, B_\eta\}$, with $A_\tau = \{\alpha_{ij}^\tau\} \in \mathbb{R}^{n\times n}$ ($\alpha_{ij}^\tau \in \mathbb{R}$) and $B_\tau = (\beta_{\tau 1}, \ldots, \beta_{\tau n})^T \in \mathbb{R}^n$; and a switching signal $\kappa : \mathbb{R}^n \to \mathcal{I} = \{1, 2, \ldots, \eta\}$ so that:

$$\dot{\mathcal{X}} = \begin{cases} A_1\mathcal{X} + B_1, & if \quad \kappa(\mathcal{X}) = 1; \\ A_2\mathcal{X} + B_2, & if \quad \kappa(\mathcal{X}) = 2; \\ \quad\vdots & \quad\quad\quad\vdots \\ A_\eta\mathcal{X} + B_\eta, & if \quad \kappa(\mathcal{X}) = \eta. \end{cases} \tag{3}$$

We can rewrite (3) in a more compact form as:

$$\dot{\mathcal{X}} = A_{\kappa(\mathcal{X})}\mathcal{X} + B_{\kappa(\mathcal{X})}. \tag{4}$$

Definition 2.3. Two η_1-PWL and η_2-PWL systems are called quasi-symmetrical if they are governed by the same linear operator $A = A_i$ for all i but $\eta_1 \neq \eta_2$.

3 System Description: one direction grid scrolls attractor

Now we assume that the dimension of each η-PWL system is $n = 3$ and that the eigenspectra of linear operators $A_\tau \in \mathbb{R}^{3\times 3}$ have the following features: a) one eigenvalue is a real number; and b) two eigenvalues are complex conjugate numbers with non-zero imaginary part. There is an approach to generate dynamical systems based on these linear dissipative systems in the case where the complex eigenvalues and the real eignenvalue have mixed sign (sometimes called an unstable dissipative system (UDS) [15]). In this paper we use a particular type of unstable dissipative system (UDS) called *Type I*:

Definition 3.1. A subsystem (A_τ, B_τ) of the system (4) in $\mathbb{R}^3$ is said to be an UDS of *Type I* if the eigenvalues of the linear operator A_τ denoted by λ_i satisfy: $\sum_{i=1}^{3} \lambda_i < 0$; λ_1 is a negative real eigenvalue and; the other two λ_2 and λ_3 are complex conjugate eigenvalues with positive real part. The system is an UDS of *Type II* if $\sum_{i=1}^{3} \lambda_i < 0$, and one λ_i is a positive real eigenvalue and; the other two λ_i are complex conjugate eigenvalues with negative real part.

To each $\tau \in \mathcal{I}$ is associated an atom $P_\tau \subset \mathbb{R}^n$, containing an equilibrium point $\chi_\tau^* = -A^{-1}B_\tau$ which has a one-dimensional stable manifold $E^s = Span\{\bar{v}_j \in \mathbb{R}^3 : \alpha_j < 0\}$ and a two-dimensional unstable manifold $E^u = Span\{\bar{v}_j \in \mathbb{R}^3 : \alpha_j > 0\}$, with $\bar{v}_j$ an eigenvector of the linear operator A and $\lambda_j = \alpha_j + i\beta_j$ its corresponding eigenvalue; *i.e.* it is a saddle equilibrium point. We are interested in bounded flows which are generated by quasi-symmetrical η-PWL systems such that for any initial condition $\mathcal{X}_0 \in \mathbb{R}^3$, the orbit $\phi(t, \chi_0)$ of the η-PWL system (4) limits to a one-spiral trajectory in the atom P_τ called a scroll. The orbit escapes from one atom to other due to the unstable manifold in each atom. In this context, the system η-PWL (4) can display various multi-scroll attractors as a result of a combination of several unstable one-spiral trajectories, while the switching between regions is governed by the function (2).

Definition 3.2. The scroll-degree of a η-PWL system (4) based on UDS *Type I* is the maximum number of scrolls that the PWL system can display in the attractor.

In this work we consider the same linear operator A, so $A_\tau = A$ for all τ. An easy approach to generate a one dimensional grid multiscroll attractor via a PWL system based on UDS type I form is by defining a double-scroll attractor as follows:

- Consider the linear operator A:

$$A = \begin{pmatrix} 0 & 1 & 0 \\ 0 & 0 & 1 \\ -\alpha_{31} & -\alpha_{32} & -\alpha_{33} \end{pmatrix}, \tag{5}$$

where α_{31}, α_{32} and α_{33} satisfy the UDS type I conditions, *i.e.*, $\lambda_1 \in \mathbb{R}$, and

$\lambda_2, \lambda_3 \in \mathbb{C}$ such that the absolute value of the imaginary part is greater than the absolute value of the real part of λ_i, with $i = 2, 3$.

- Choose two equilibria on the x-axis: $\chi_1^* = (x_{eq1}^*, 0, 0)^T$ and $\chi_2^* = (x_{eq2}^*, 0, 0)^T$.
- Compute the stable and unstable manifolds E_1^s, E_1^u, E_2^s, and E_1^u associated to each equilibria χ_1^* and χ_2^*, respectively.
- Find the intersection points between the stable manifold E_1^s and the unstable manifold E_2^u, and between the stable manifold E_2^s and the unstable manifold E_1^u.
- Define the switching surface as the plane that pass through the intersection points $E_1^s \cap E_2^u$, and $E_2^s \cap E_1^u$ and the line: $x_1 = (x_{eq1}^* + x_{eq2}^*)/2$, $x_3 = 0$.
- Compute the constant vectors $B_\tau = -A\chi_\tau^*$, with $\tau = 1, 2$.

The above steps generate two heteroclinic orbits between the equilibria χ_1^* and χ_2^*. One of the heteroclinic orbits is from χ_1^* to the point $E_2^s \cap E_1^u$ and from this point to χ_2^*. The other heteroclinic orbit is from χ_2^* to the point $E_1^s \cap E_2^u$ and from this point to χ_1^*.

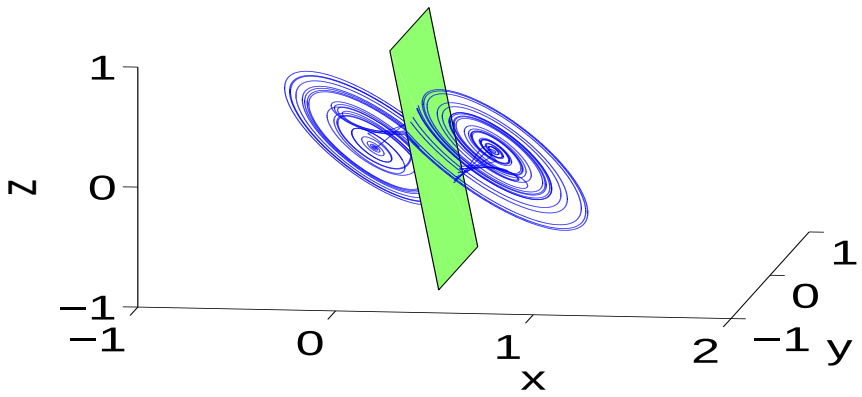

Figure 1: Attractor generated by the PWL system given by the linear operator (5), The vectors $B_1 = (0, 0, 0)^T$ and $B_2 = (0, 0, 0.9)^T$ and switching surface $\{\mathcal{X} \in \mathbb{R}^3 : 0.7369x_1 + 0.0918x_3 - 0.2211 = 0\}$ (green plane).

In order to illustrate the approach to generate double-scroll attractors using (4), we set $\alpha_{31} = 1.5$, $\alpha_{32} = 1$ and $\alpha_{33} = 1$.

- Thus, the eigenvalues are $\lambda_1 = -1882/1563$, $\lambda_2 = 319/3126 + 2503/2252i$, and $\lambda_2 = 319/3126 - 2503/2252i$ which satisfy: $\sum_{i=1}^{3} \lambda_i < 0$ and $Imag(\lambda_2)/Re(\lambda_2) > 6$. $Imag(\lambda_2)$ and $Re(\lambda_2)$ denote the imaginary part and real part of λ_2, respectively.

- Choose equilibra at $\chi_1^* = (0,0,0)^T$ and $\chi_2^* = (0.6,0,0)^T$.
- The unstable manifolds $E_1^u = \{\mathcal{X} \in \mathbb{R}^3 : 0.3646x_1 - 0.0597x_2 + 0.2927x_3 = 0\}$ and $E_2^u = \{\mathcal{X} \in \mathbb{R}^3 : 0.3646x_1 - 0.0597x_2 + 0.2927x_3 - 0.2188 = 0\}$ and the stable manifolds $E_1^s = \{\mathcal{X} \in \mathbb{R}^3 : \frac{x_1}{-0.4687} = \frac{x_2}{0.5644} = \frac{x_3}{-0.6796}\}$ and $E_2^s = \{\mathcal{X} \in \mathbb{R}^3 : \frac{x_1-0.6}{-0.4687} = \frac{x_2}{0.5644} = \frac{x_3}{-0.6796}\}$
- $E_1^s \cap E_2^u = (0.2541, -0.3060, 0.3684)^T$, and $E_2^s \cap E_1^u = (0.3459, -0.3060, -0.3684)^T$ and the line: $x_1 = 0.3$, $x_2 \in \mathbb{R}$, $x_3 = 0$. So the switching surface is given by $\{\mathcal{X} \in \mathbb{R}^3 : 0.7369x_1 + 0.0918x_3 - 0.2211 = 0\}$.
- $B_1 = -A\chi_1^* = (0,0,0)^T$ and $B_2 = -A\chi_2^* = (0,0,0.9)^T$.

The calculated values approximate the exact values needed for the heteroclinic orbit and they allow us to generate a double-scroll attractor by trapping the trajectories oscillating around the equilibria, see Figure 1.

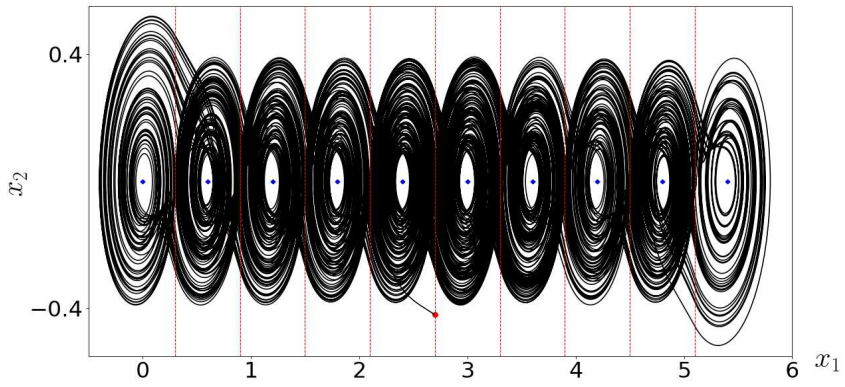

Figure 2: Projection of the attractor generated by the quasi-symmetrical 10-PWL(S) system onto the (x_1, x_2) plane. The dashed lines mark the division between the atoms.

Example 3.3. In order to illustrate the generation of multiscroll attractors using (4), we consider a quasi-symmetrical 10-PWL system defined in $\mathbb{R}^3$ with state vector $\mathcal{X} = (x_1, x_2, x_3)^T$ and linear operator defined as follows

$$A = \begin{pmatrix} 0 & 1 & 0 \\ 0 & 0 & 1 \\ -\alpha_{31} & -\alpha_{32} & -\alpha_{33} \end{pmatrix}; \tag{6}$$

where $\alpha_{31} = 1.5, \alpha_{32} = 1$ and $\alpha_{33} = 1$; the set of constants vectors

$$\mathbf{B} = \{B_1 = (0,0,0)^T, B_2 = (0,0,0.9)^T, B_3 = (0,0,1.8)^T, B_4 = (0,0,2.7)^T,$$

$$B_5 = (0,0,3.6)^T, B_6 = (0,0,4.5)^T, B_7 = (0,0,5.4)^T, B_8 = (0,0,6.3)^T,$$
$$B_9 = (0,0,7.2)^T, B_{10} = (0,0,8.1)^T\};$$

and the partition:

$$\begin{aligned}\mathcal{P} \;=\; \{\; & P_1 = \{\mathcal{X} \in \mathbf{R}^3 : x_1 < 0.3\}, P_2 = \{\mathcal{X} \in \{\mathcal{X} \in \mathbf{R}^3 : 0.3 \leq x_1 < 0.9\}, \\ & P_3 = \{\mathcal{X} \in \mathbf{R}^3 : 0.9 \leq x_1 < 1.5\}, P_4 = \{\mathcal{X} \in \mathbf{R}^3 : 1.5 \leq x_1 < 2.1\}, \\ & P_5 = \{\mathcal{X} \in \mathbf{R}^3 : 2.1 \leq x_1 < 2.7\}, P_6 = \{\mathcal{X} \in \mathbf{R}^3 : 2.7 \leq x_1 < 3.3\}, \\ & P_7 = \{\mathcal{X} \in \mathbf{R}^3 : 3.3 \leq x_1 < 3.9\}, P_8 = \{\mathcal{X} \in \mathbf{R}^3 : 3.9 \leq x_1 < 4.5\} \\ & P_9 = \{\mathcal{X} \in \mathbf{R}^3 : 4.5 \leq x_1 < 5.1\}, P_{10} = \{\mathcal{X} \in \mathbf{R}^3 : x_1 \geq 5.1\}\}\end{aligned} \tag{7}$$

The eigenvalues of A are $\lambda_1 = -1.20$ and $\lambda_{2,3} = 0.10 \pm 1.11i$. By Definition 2.4, the system is an UDS of *Type I*. The equilibrium points for this system are at $\chi_1^* = (0,0,0)^T$, $\chi_2^* = (0.6,0,0)^T$, $\chi_3^* = (1.2,0,0)^T$, $\chi_4^* = (1.8,0,0)^T$, $\chi_5^* = (2.4,0,0)^T$, $\chi_6^* = (3,0,0)^T$, $\chi_7^* = (3.6,0,0)^T$, $\chi_8^* = (4.2,0,0)^T$, $\chi_9^* = (4.8,0,0)^T$ and $\chi_{10}^* = (5.4,0,0)^T$. Figure (2) depicts the projection of the attractor generated by the quasi-symmetrical 10-PWL(S) system onto the (x_1, x_2) plane with initial condition $\chi_0 = (2.7, -0.42, 0.09)^T$. We solved this system (3) numerically by using fourth order Runge-Kutta method with $2,000,000$ time iterations and step-size $h = 0.01$ in order to corroborate that the system always oscillates in the attractor and for the initial condition considered the asymptotic regime is achieved after 5000 iterations. When we refer to 2000 arbitrary units of time correspond to 200,000 iterations.

The trajectory $\mathcal{X}(t)$ of the PWL system can be calculated by $\mathcal{X}^i(t) = e^{At}\mathcal{X}_0^i$ in each atom P_i, where $\mathcal{X}^i = \mathcal{X} + \mathcal{X}_i^*$ and $\mathcal{X}_0^i$ is the initial condition when the trajectory enter to the atom P_i, $i = 1, \ldots, 10$. Then

$$\mathcal{X}^i(t) = PE(t)P^{-1}\mathcal{X}^i(0),$$

where P is the invertible matrix defined by the eigenvector of A and

$$E(t) = \begin{pmatrix} e^{\lambda_1 t} & 0 & 0 \\ 0 & e^{Re(\lambda_2)t}\sin(Imag(\lambda_2)t) & -e^{Re(\lambda_2)t}\cos(Imag(\lambda_2)t) \\ 0 & e^{Re(\lambda_2)t}\cos(Imag(\lambda_2)t) & e^{Re(\lambda_2)t}\sin(Imag(\lambda_2)t) \end{pmatrix}.$$

4 Symbolic dynamics of trajectories of a pair of coupled PWL systems

Consider a pair of quasi-symmetrical η-PWL systems defined by (4), *i.e.*, they have different scroll-degrees. They are coupled in a Master-Slave configuration as follows.

$$\begin{aligned}\dot{\mathcal{X}}_m &= A\mathcal{X}_m + B_{\kappa_m(\mathcal{X}_m)}, \\ \dot{\mathcal{X}}_s &= A\mathcal{X}_s + B_{\kappa_s(\mathcal{X}_s)} + c\Gamma(\mathcal{X}_m - \mathcal{X}_s),\end{aligned} \tag{8}$$

where $\mathcal{X}_m = (x_1^m, x_2^m, x_3^m)^T$ and $\mathcal{X}_s = (x_1^s, x_2^s, x_3^s)^T$ are the state vectors of the master and slave systems, respectively. $\mathcal{X}_m$ is in the phase space of the

master system D_m; $\mathcal{X}_s$ is in the phase space D_s. Clearly the orbits of the overall system lie in a subspace of the whole state space $D_m \oplus D_s$. $\kappa_i : \mathbb{R}^3 \to \mathcal{I}_i = \{1, 2, \ldots, \eta_i\}$, with $i = m, s$ and $\eta_m \neq \eta_s$, is the signal of the master system ($i = m$) and slave system ($i = s$). The itineraries generated by τ of the master and slave systems are $\mathcal{S}_m(\mathcal{X}_{m0}) = \{\tau_0, \tau_1, \ldots\}$ and $\mathcal{S}_s(\mathcal{X}_{s0}) = \{\tau'_0, \tau'_1, \ldots\}$, respectively. The corresponding time sets are given by $\Delta_{tm} = \{t_0, t_1, \ldots\}$ and $\Delta_{ts} = \{t'_0, t'_1, \ldots\}$. We take the constant matrix $\Gamma = \text{diag}\{r_1, r_2, r_3\} \in \mathbb{R}^{3\times 3}$ to be the inner linking matrix where $r_l = 1$ (for $l = 1, 2, 3$) if both master and slave systems are linked through their l-th state variable, and $r_l = 0$ otherwise. The parameter $0 < c \in \mathbb{R}$ is the coupling strength.

There are several definitions of synchronization [16, 18], for instance, complete synchronization is given as follows:

Definition 4.1. The master-slave system (4) is said to achieve complete synchronization if

$$\lim_{t\to\infty} ||\phi_m(t, \mathcal{X}_{m0}) - \phi_s(t, \mathcal{X}_{s0})|| \to 0. \tag{9}$$

for all initial conditions, $\mathcal{X}_{m0}$ and $\mathcal{X}_{s0}$.

The symbol $||\cdot||$ denotes the Euclidean distance in $\mathbb{R}^3$. This mode of synchronization is very strong. There are weaker and more generalized notions of synchronization [17]. Suppose that $\mathcal{F}$ is a transformation from the trajectories of the attractor in D_m space to the trajectories in D_s space. The precise form of $\mathcal{F}$ will depend upon the application in mind. Given such a transformation, Generalized Synchronization is defined as follows.

Definition 4.2. The master-slave system (4) is said to achieve generalized synchronization if

$$\lim_{t\to\infty} ||\mathcal{F}((\phi_m(t, \mathcal{X}_{m0})) - \phi_s(t, \mathcal{X}_{s0})|| \to 0. \tag{10}$$

for all $\mathcal{X}_{m0}$ and $\mathcal{X}_{s0}$ where $\mathcal{F}$ is the given transformation from the trajectories of the attractor in D_m space to the trajectories in D_s space.

It has been reported in [12] that in the type of configuration given by (8) the master system determines the scroll-degree in the slave system. In particular, if $\eta_m < \eta_s$, then the master-slave system achieves generalized synchronization and $\eta_s - \eta_m + 1$different basins of attraction appear. The trajectories of the slave system depend on their initial condition. That is, the master-slave configuration results in multiple basins of attraction for the slave. This phenomenon is called multistability [19]. On the other hand, if $\eta_m > \eta_s$, then the slave system increases its scroll-degree till it matches the master's scroll-degree.

In order to illustrate the dynamical behavior of the master-slave system, consider two quasi-symmetrical η-PWL systems with common linear operator A and a set of constant vectors $\mathbf{B} = \{B_3, B_4, \ldots, B_{10}\}$ defined in Example 3.3 (Eq. (6)).

Example 4.3. As a first example of a coupled pair of multiscroll chaotic systems, suppose that the master's scroll-degree is $\eta_m = 3$ and the slave's scroll-degree is $\eta_s = 8$, and both are connected with a coupling strength c and an

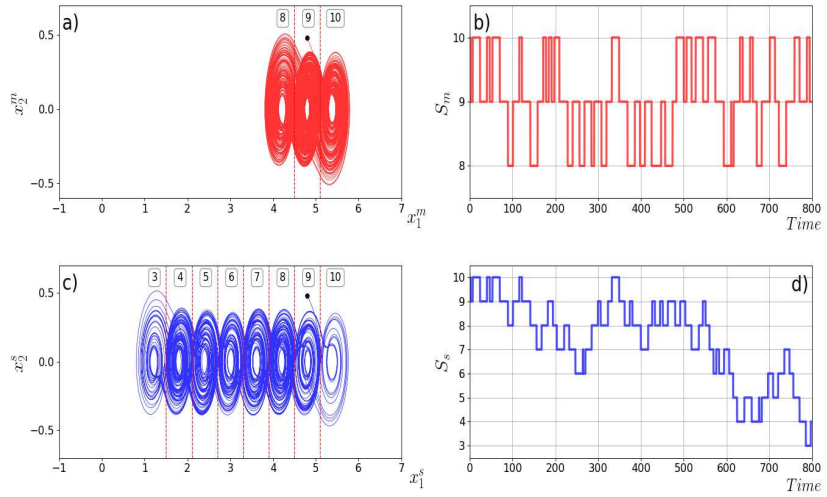

Figure 3: a) Projection of the master system onto the plane (x_1^m, x_2^m) with initial condition $\chi_{mo} = (4.8, 0.48, -0.29)^T$; b) The master itinerary $S_m(\chi_{m0})$; c) Projection of the slave system onto the plane (x_1^s, x_2^s) with initial condition $\chi_{so} = (4.8, 0.48, -0.29)^T$, for coupling strength $c = 0$; d) The slave itinerary $S_s(\chi_{s0})$.

inner coupling matrix given by $\Gamma = \{0, 1, 0\}$. The signal for the master system $\kappa_m : \mathbb{R}^3 \to \mathcal{I}_m = \{8, 9, 10\}$ is

$$\kappa_m(\mathcal{X}) = \begin{cases} 10, & \text{if} \quad \mathcal{X} \in P_{10} = \{\mathcal{X} \in \mathbb{R}^3 : x_1 \geq 5.1\}; \\ 9, & \text{if} \quad \mathcal{X} \in P_9 = \{\mathcal{X} \in \mathbb{R}^3 : 4.5 \leq x_1 < 5.1\}; \\ 8, & \text{if} \quad \mathcal{X} \in P_8 = \{\mathcal{X} \in \mathbb{R}^3 : x_1 < 4.5\}. \end{cases} \tag{11}$$

And for the slave system the function $\kappa_s : \mathbb{R}^3 \to \mathcal{I}_s = \{3, 4, \ldots, 10\}$ is

$$\kappa_s(\mathcal{X}) = \begin{cases} 10, & \text{if} \quad \mathcal{X} \in P_{10} = \{\mathcal{X} \in \mathbb{R}^3 : x_1 \geq 5.1\}; \\ 9, & \text{if} \quad \mathcal{X} \in P_9 = \{\mathcal{X} \in \mathbb{R}^3 : 4.5 \leq x_1 < 5.1\}; \\ 8, & \text{if} \quad \mathcal{X} \in P_8 = \{\mathcal{X} \in \mathbb{R}^3 : 3.9 \leq x_1 < 4.5\}; \\ 7, & \text{if} \quad \mathcal{X} \in P_7 = \{\mathcal{X} \in \mathbb{R}^3 : 3.3 \leq x_1 < 3.9\}; \\ 6, & \text{if} \quad \mathcal{X} \in P_6 = \{\mathcal{X} \in \mathbb{R}^3 : 2.7 \leq x_1 < 3.3\}; \\ 5, & \text{if} \quad \mathcal{X} \in P_5 = \{\mathcal{X} \in \mathbb{R}^3 : 2.1 \leq x_1 < 2.7\}; \\ 4, & \text{if} \quad \mathcal{X} \in P_4 = \{\mathcal{X} \in \mathbb{R}^3 : 1.5 \leq x_1 < 2.1\}; \\ 3, & \text{if} \quad \mathcal{X} \in P_3 = \{\mathcal{X} \in \mathbb{R}^3 : x_1 < 1.5\}. \end{cases} \tag{12}$$

Using Runge-Kutta with 200000 time iterations and a step-size of $h = 0.01$, we numerically solve the system (8). Firstly, we analyze the particular case when the coupling strength is $c = 0$, the systems are not coupled. Projections of the attractors onto the planes (x_1^m, x_2^m) and (x_1^s, x_2^s) are given in Figures 3 a) and c), in both cases the master and slave systems start at the same initial condition $\chi_{m0} = \chi_{s0} = (4.8, 0.48, -0.29)^T$. This initial condition is indicated

with a black dot in figures. The master and slave systems oscillate in a different way since they have different scroll degrees $\eta_m = 3$ and $\eta_s = 8$. The elements of the index sets $\mathcal{I}_m = \{8, 9, 10\}$ and $\mathcal{I}_s = \{3, 4, 5, 6, 7, 8, 9, 10\}$ for the master and slave systems, respectively, are indicated on the top of Figures 3 a) and c).

Figures 3 b) and d) show the itineraries $S_m(\chi_{m0})$ and $S_s(\chi_{s0})$ of the master and slave systems, respectively. Note that they are different because the systems have different scroll-degrees, even though they start at the same initial condition. The itineraries $S_m(\chi_{m0})$ and $S_s(\chi_{s0})$ are given by the dynamics of the master and slave systems and correspond to the activation of the systems in different atoms of the partitions, *i.e.*, the itinerary $S_m(\chi_{m0})$ generated by $\kappa_m : \mathbb{R}^3 \to \mathcal{I}_m$ only takes three values $\{8, 9, 10\}$, meanwhile the itinerary $S_s(\chi_{s0})$ is generated by $\kappa_s : \mathbb{R}^3 \to \mathcal{I}_s$ and takes eight values $\{3, 4, 5, 6, 7, 8, 9, 10\}$.

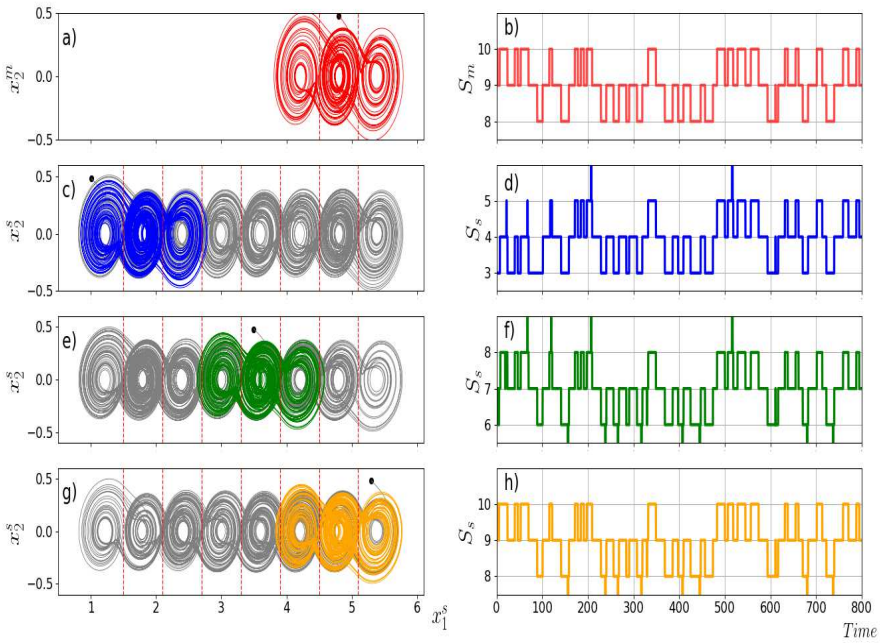

Figure 4: Projections of the master and slave systems onto the (x_1^m, x_2^m) plane and the (x_1^s, x_2^s) plane, respectively, for $\eta_m = 3$, $\eta_s = 8$, $\Gamma = \{0, 1, 0\}$ and coupling strength $c = 10$. a) Master system with initial condition $\chi_{mo} = (4.8, 0.48, -0.29)^T$ and b) its itinerary $\mathcal{S}_m(\mathcal{X}_{mo})$. Slave system with different initial conditions: c) $\chi_{so1} = (1.01, 0.48, -0.29)^T$, and d) its itinerary $\mathcal{S}_s(\mathcal{X}_{so1})$. e) $\chi_{so2} = (3.5, 0.48, -0.29)^T$ and f) its itinerary $\mathcal{S}_s(\mathcal{X}_{so2})$. g) $\chi_{so3} = (5.3, 0.48, -0.29)^T$ and h) its itinerary $\mathcal{S}_s(\mathcal{X}_{so3})$.

Now, we set the coupling strength $c = 10$ and use different initial conditions for the slave system. The matriz $A - c\Gamma$ is Hurwitz for $0.2 < c$, with this in mind we choose arbitrarily the coupling strength $c = 10$ to drive the slave system by the master system.

Figure 4 shows the projections of master-slave system given by (8) onto the planes (x_1^m, x_2^m) and (x_1^s, x_2^s). Different initial conditions are used for the slave system located at distinct atoms. For the master system the initial condition is $\chi_{mo} = (4.8, 0.48, -0.29)^T$, see Figure 4 a). Specifically we use different initial conditions for the slave system $\chi_{so1} = (1.01, 0.48, -0.29)^T$ for Figure 4 c), $\chi_{so2} = (3.5, 0.48, -0.29)^T$ for Figure 4 e) and $\chi_{so3} = (5.3, 0.48, -0.29)^T$ for Figure 4 g). It is worthwhile to observe that the slave system reduces its scroll-degree to three and, depending on the initial condition, it evolves between distinct basins of attraction and multistability appears. We plot in gray the trajectory of the slave system when it is not coupled with the master system in order to compare it when it is coupled, see Figure 4 c), e) and g).

Notice that the itinerary of the master system $S_m(\chi_{m0})$ generated by $\kappa_m : \mathbb{R}^3 \to \mathcal{I}_m = \{8, 9, 10\}$ remains, however the itinerary of the slave system $S_m(\chi_{m0})$ generated by $\kappa_s : \mathbb{R}^3 \to \mathcal{I}_s$ is determined by its initial condition, for instance, the itinerary takes different values according to the atom where the initial condition belongs $\chi_{s0} \in P_i$, for $i = 3, \ldots, 10$. Now the itinerary of the slave system is restricted to take a subset of the index set $\mathcal{I}_s$, *i.e.*, $\mathcal{I}_s(\chi_{s0}) \subset \mathcal{I}_s$ which will be called restricted index set. This is because the number of scrolls that the slave system coupled with $c = 10$ displays less scrolls that when it is not coupled. Thus the restricted index sets have different cardinality that is determined by the initial condition $\chi_{s0} \in P_i$, for $i = 3, \ldots, 10$. So for these three initial conditions there are three different restricted index sets given as follows:

$$\kappa_s : \mathbb{R}^3 \to \mathcal{I}_s(\chi_{s0}) \subset \mathcal{I}_s = \begin{cases} \mathcal{I}_s(\chi_{s01}) = \{3, 4, 5, 6\}, \\ \mathcal{I}_s(\chi_{s02}) = \{5, 6, 7, 8, 9\}, \\ \mathcal{I}_s(\chi_{s03}) = \{7, 8, 9, 10\}. \end{cases}$$

The cardinality of the index set $\mathcal{I}_m$, and the restricted index sets $\mathcal{I}_s(\chi_{s01})$, $\mathcal{I}_s(\chi_{s02})$ and $\mathcal{I}_s(\chi_{s03})$ are $3, 4, 5$, and 4, respectively.

There is a problem if we want to detect similar behaviour under the presence of multistability . The inconvenience is resolved by means of defining a new itinerary based on the trajectory of the systems instead of the dynamics.

Let $\mathcal{I}_B = \{\#_1, \ldots, \#_n\}$ be an index set that labels each element of a partition $P_\phi = \{P_1', \ldots, P_n'\}$ of the basin of attraction of a dynamical system with flow ϕ. A function $\kappa : \mathbb{R}^n \to \mathcal{I}_B$ of the form

$$\kappa(\phi(t, \chi_0)) = \begin{cases} \#_1, \text{ if } \phi(t, \chi_0) \in P_1'; \\ \#_2, \text{ if } \phi(t, \chi_0) \in P_2'; \\ \vdots \\ \#_n, \text{ if } \phi(t, \chi_0) \in P_n'; \end{cases}$$

generates an itinerary of the trajectory. If $\kappa(\phi(\chi_0)) = s_i \in \mathcal{I}_B$ during the time interval $t \in [t_i, t_{i+1})$, then $S^\phi(\chi_0) = \{s_0, s_1, s_2, \ldots\}$ stands for the itinerary of the trajectory $\phi(\chi_0)$.

In our setting in order to describe appropriately the flows of a master-slave system via symbolic dynamics it is necessary to consider additional atoms $P_{-n}, \ldots, P_0$, and $P_{\eta+1}, \ldots, P_N$ at the 'ends' of the contiguous partition atoms

to account for exits and returns to P_1 and P_η, respectively, to the partition $\mathcal{P} = \{P_1, \ldots, P_\eta\}$. So we code according to the partition $\mathcal{P}_\phi = \{P_{-n}, \ldots, P_0, P_1, \ldots, P_\eta, P_{\eta+1}, \ldots, P_N\}$. We obtain a symbolic trajectory by writing down the sequence of symbols corresponding to the successive partition elements visited by the trajectory during a certain period of time.

We are interested when the trajectories oscillate in the attractor, so it is enough to consider a new partition with two atoms P_0 and $P_{\eta+1}$ next to the atoms P_1 and P_η, *i.e.*, $\mathcal{P}_\phi = \{P_0, P_1, P_2, \ldots, P_\eta, P_{\eta+1}\}$. So the partition $\mathcal{P}_\phi$ has been obtained by adding two atoms P_0 and $P_{\eta+1}$ to the partition $\mathcal{P}$ as follows:

- The atoms $P_i \in \mathcal{P}_\phi$, for $i = 2, \ldots, \eta - 1$, are the same that the atoms $P_i \in \mathcal{P}$, for $i = 2, \ldots, \eta - 1$. These atoms are given by the switching surfaces $v^T\mathcal{X} = \delta_i$, $i = 1, \ldots, \eta - 1$ with $\delta_2 - \delta_1 = \delta_3 - \delta_2 = \ldots = \delta_{\eta-1} - \delta_{\delta-2}$.
- The atoms $P_1, P_\eta \in \mathcal{P}_\phi$ are given by $P_1 = \{\mathcal{X} \in \mathbb{R}^n : \delta_0 \leq v^T\mathcal{X} < \delta_1\}$, and $P_\eta = \{\mathcal{X} \in \mathbb{R}^n : \delta_{\eta-1} \leq v^T\mathcal{X} < \delta_\eta\}$, such that $\delta_1 - \delta_0 = \delta_2 - \delta_1 = \delta_\eta - \delta_{\eta-1}$.
- The atoms P_0 and $P_{\eta+1}$ are given by fulfilling $\bigcup_{i=0}^{\eta+1} P_i = \mathbb{R}^n$.

For simplicity we generate a new partition $\mathcal{P}_\phi = \{P_2, P_3, \ldots, P_{10}, P_{11}\}$ based on the partition $\mathcal{P} = \{P_3, \ldots, P_{10}\}$ which was considered by equation (12), because the flow $\phi(\chi_0) \subset P_\phi$ and the index sets present the same cardinality.

The partition $\mathcal{P}_\phi$ is given as follows:

$$\begin{aligned}\mathcal{P}_\phi \;=\; \{\; & P_2 = \{\mathcal{X} \in \mathbf{R}^3 : x_1 < 0.9\},\\ & P_3 = \{\mathcal{X} \in \mathbf{R}^3 : 0.9 \leq x_1 < 1.5\}, P_4 = \{\mathcal{X} \in \mathbf{R}^3 : 1.5 \leq x_1 < 2.1\},\\ & P_5 = \{\mathcal{X} \in \mathbf{R}^3 : 2.1 \leq x_1 < 2.7\}, P_6 = \{\mathcal{X} \in \mathbf{R}^3 : 2.7 \leq x_1 < 3.3\},\\ & P_7 = \{\mathcal{X} \in \mathbf{R}^3 : 3.3 \leq x_1 < 3.9\}, P_8 = \{\mathcal{X} \in \mathbf{R}^3 : 3.9 \leq x_1 < 4.5\},\\ & P_9 = \{\mathcal{X} \in \mathbf{R}^3 : 4.5 \leq x_1 < 5.1\}, P_{10} = \{\mathcal{X} \in \mathbf{R}^3 : 5.1 \leq x_1 < 5.7\},\\ & P_{11} = \{\mathcal{X} \in \mathbf{R}^3 : 5.7 \leq x_1\}\}.\end{aligned} \tag{13}$$

Thus $\mathcal{S}_m^\phi(\mathcal{X}_{m0}) = \{s_0, s_1, \ldots, s_m, \ldots\}$ stands for the itinerary generated by the trajectory of the master system $\phi_m(t, \mathcal{X}_{m0})$ at $\mathcal{X}_{m0}$ and, $\mathcal{S}_m^\phi(i, \mathcal{X}_{m0})$ is the element $s_i \in \mathcal{S}_m^\phi(\mathcal{X}_0)$ that occurs at time t_i, so the set $\Delta_{\phi_m} = \{t_0, t_1, \ldots, t_m, \ldots\}$ is generated. In a similar way, we can define the itinerary, $\mathcal{S}_s^\phi(\mathcal{X}_{s0})$ and the set $\Delta_{\phi_s} = \{t'_0, t'_1, \ldots, t'_m, \ldots\}$ generated by the trajectory of the slave system. We always assume that the initial conditions belong to their respectively basin of attraction of the system.

Thereafter, the master index set $\mathcal{I}_m$ and restricted index sets $\mathcal{I}_s(\chi_{s01})$, $\mathcal{I}_s(\chi_{s02})$ and $\mathcal{I}_s(\chi_{s03})$ have the same cardinality independently of the initial conditions $\chi_{s0} \in P_i$, for $i = 3, \ldots, 10$. Now for these three initial conditions there are three different restricted index sets with the same cardinality given as follows:

$$\kappa_s : \mathbb{R}^3 \to \mathcal{I}_s(\chi_{s0}) \subset \mathcal{I}_s = \begin{cases} \mathcal{I}_s(\chi_{s01}) = \{2, 3, 4, 5, 6\}, \\ \mathcal{I}_s(\chi_{s02}) = \{5, 6, 7, 8, 9\}, \\ \mathcal{I}_s(\chi_{s03}) = \{7, 8, 9, 10, 11\}. \end{cases} \tag{14}$$

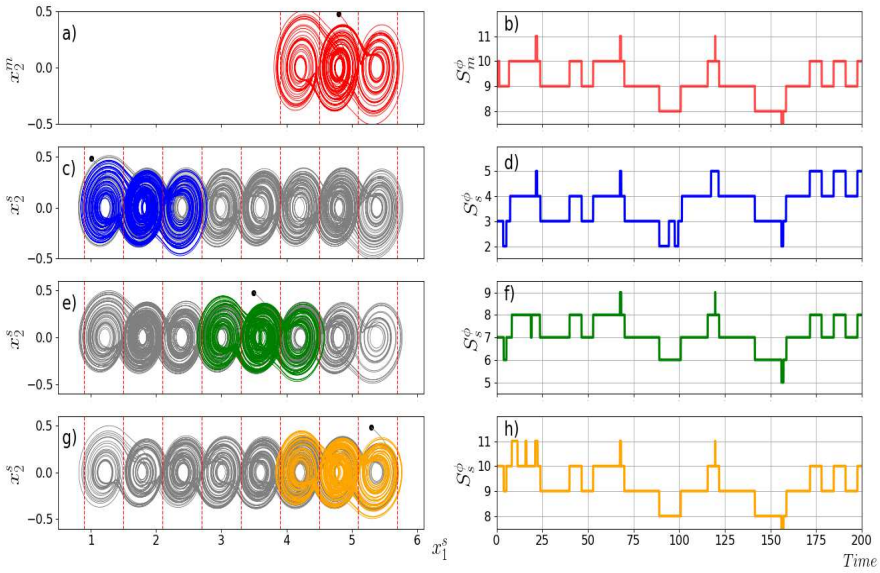

Figure 5: Projections of the master and slave systems onto the (x_1^m, x_2^m) plane and the (x_1^s, x_2^s) plane, respectively, for $\eta_m = 3$, $\eta_s = 8$, $\Gamma = \{0, 1, 0\}$ and coupling strength $c = 10$. a) Master system with initial condition $\chi_{mo} = (4.8, 0.48, -0.29)^T$ and b) its itinerary $\mathcal{S}_m(\mathcal{X}_{mo})$. Slave system with different initial conditions: c) $\chi_{so1} = (1.01, 0.48, -0.29)^T$, and d) its itinerary $\mathcal{S}_s(\mathcal{X}_{so1})$. e) $\chi_{so2} = (3.5, 0.48, -0.29)^T$ and f) its itinerary $\mathcal{S}_s(\mathcal{X}_{so2})$. g) $\chi_{so3} = (5.3, 0.48, -0.29)^T$ and h) its itinerary $\mathcal{S}_s(\mathcal{X}_{so3})$.

And for the master index set:

$$\kappa_m : \mathbb{R}^3 \to \mathcal{I}_m = \{7, 8, 9, 10, 11\}.$$

The cardinality of all of the index set and restricted index sets $\mathcal{I}_m$, $\mathcal{I}_s(\chi_{s01})$, $\mathcal{I}_s(\chi_{s02})$ and $\mathcal{I}_s(\chi_{s03})$ is 5. Figure 5 a) shows the projection of the master attractor onto the plane (x_1^m, x_2^m) and the atoms of P_ϕ are marked. Figure 5 c), e) and g) shows the projection of the slave attractor onto the plane (x_1^s, x_2^s) for different initial conditions and the atoms of P_ϕ are marked. In Figure 5 b) we show the itinerary of the master system $\mathcal{S}_m^\phi(\mathcal{X}_{m0})$ and in Figures 5 d), 5 f) and 5 h) the itinerary of the slave system by varying the initial condition. Notice that the itinerary of the trajectory of the master system and the three itineraries of the trajectories of the slave system for different initial conditions visit five different domains. Figure 6 shows three signals which were generated by the difference between the master itinerary $\mathcal{S}_m^\phi(i, \chi_{m_0})$ and slave itineraries for different initial conditions $\mathcal{S}_s^\phi(i, \chi_{s0})$, with $\chi_{s0} = \{\chi_{s0_1}, \chi_{s0_2}, \chi_{s0_3}\}$. These signals are comprised of spikes and a constant offset k, the spikes correspond to when the trajectory goes from one atom to other and the constant offset is produced because the index set $\mathcal{I}_m$ and restricted index sets $\mathcal{I}_s(\chi_{s01})$, $\mathcal{I}_s(\chi_{s02})$ and $\mathcal{I}_s(\chi_{s03})$ are given by different symbols. The constant offsets k_i, $i = 1, 2, 3$, by which the average

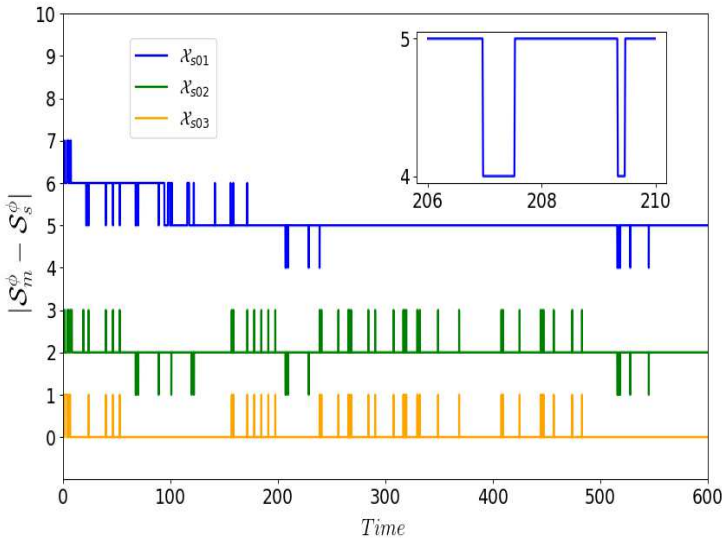

Figure 6: Difference between the itineraries of the master and the slave systems for the initial conditions given in the example 4.3. The inner sub-figure shows a zoom of the blue signal for a short period of time.

value of the difference signal is not centered around the t-axis is computed by the $k_i = |min\{\mathcal{I}_m\} - min\{\mathcal{I}_{soi}\}|$, where $min\{\mathcal{I}_j\}$ means the minimum value of the set $\mathcal{I}_j$. For the initial condition $\chi_{s01} = (1.01, 0.48, -0.29)^T$ determines the constant offset $k_1 = 5$, $\chi_{s02} = (3.5, 0.48, -0.29)^T$ determines the constant offset $k_2 = 2$ and $\chi_{s03} = (5.3, 0.48, -0.29)^T$ determines $k_3 = 0$. The constant offset $k_3 = 0$ is because the index set $\mathcal{I}_m$ and the restricted index set $\mathcal{I}_{s03}$ are comprised by the same symbols $\{7, 8, 9, 10, 11\}$. If we relabeled the partition atoms to make the restricted index sets $\mathcal{I}_{s01}$ and $\mathcal{I}_{s02}$ be equal to $\mathcal{I}_{s03}$, then all the constant offsets k_1, k_2 and k_3 will be zero.

5 Itinerary synchronization

In the context of synchronization and multistability, we propose the following definition of synchronization based on the itinerary of trajectories in multiscroll attractors:

Definition 5.1. The master-slave system (8) is said to achieve itinerary synchronization if after relabeling the partition atoms

$$\lim_{i\to\infty} |\mathcal{S}_m^\phi(i, \mathcal{X}_{m0}) - \mathcal{S}_s^\phi(i, \mathcal{X}_{s0})| = 0, \tag{15}$$

for all initial conditions $\mathcal{X}_{m0}$ and $\mathcal{X}_{s0}$ in the basin of attraction.

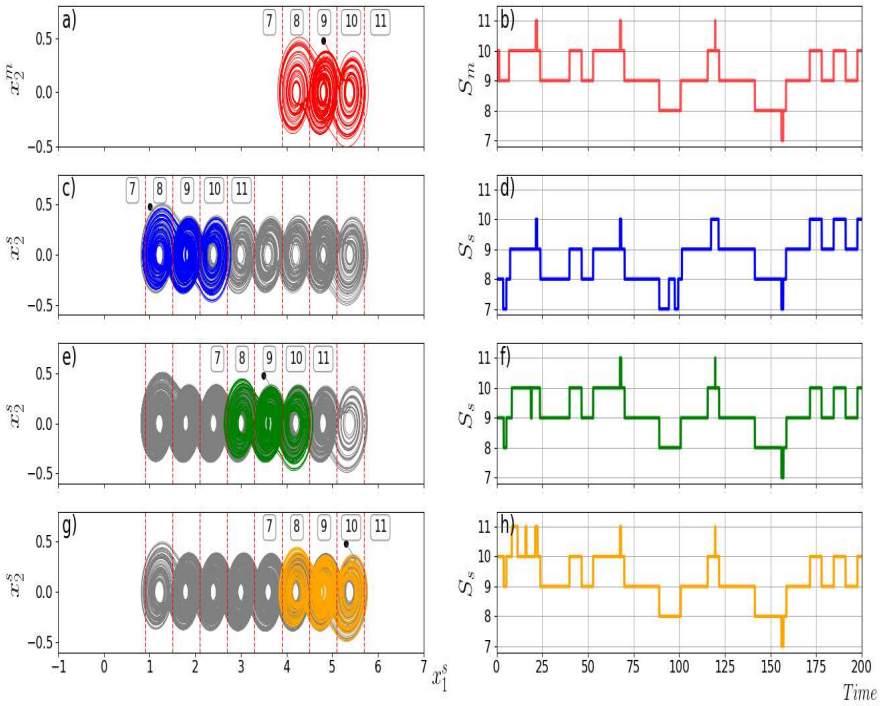

Figure 7: Projections of the master and slave systems onto the (x_1^m, x_2^m) plane and the (x_1^s, x_2^s) plane, respectively, for $\eta_m = 3$, $\eta_s = 8$, $\Gamma = \{0, 1, 0\}$ and coupling strength $c = 10$. a) Master system with initial condition $\chi_{m0} = (4.8, 0.48, -0.29)^T$ and b) its itinerary $\mathcal{S}_m(\mathcal{X}_{m0})$. Slave system with different initial conditions: c) $\chi_{s01} = (1.01, 0.48, -0.29)^T$, and d) its itinerary $\mathcal{S}_s(\mathcal{X}_{so1})$ after it was relabeled. e) $\chi_{s02} = (3.5, 0.48, -0.29)^T$ and f) its itinerary $\mathcal{S}_s(\mathcal{X}_{s02})$ after it was relabeled. g) $\chi_{s03} = (5.3, 0.48, -0.29)^T$ and h) its itinerary $\mathcal{S}_s(\mathcal{X}_{s03})$ without being relabeled.

The definition of itinerary synchronization is meant to capture the idea that knowing the itinerary of one sequence determines precisely the itinerary of the other (after relabeling). Clearly itinerary synchronization will hold if the master-slave system (8) presents complete synchronization with the same scroll-degree for the master system and slave system since the trajectories of the master and slave system will visit the same atoms at the same time.

The process of relabeling is shown in Figure 7, here it is possible to see that the atoms where the slave system oscillates were relabeled according to the master system and we can compare the itineraries between the master and slave system. In Figure 7 b) we show the itinerary of the master system $\mathcal{S}_m^{\phi}(\mathcal{X}_{m0})$ and in Figures 7 d), 7 f) and 7 h) the itinerary of the slave system corresponding to various initial conditions, $\chi_{s01} = (1.01, 0.48, -0.29)^T$, $\chi_{s02} = (3.5, 0.48, -0.29)^T$ and $\chi_{s03} = (5.3, 0.48, -0.29)^T$, respectively.

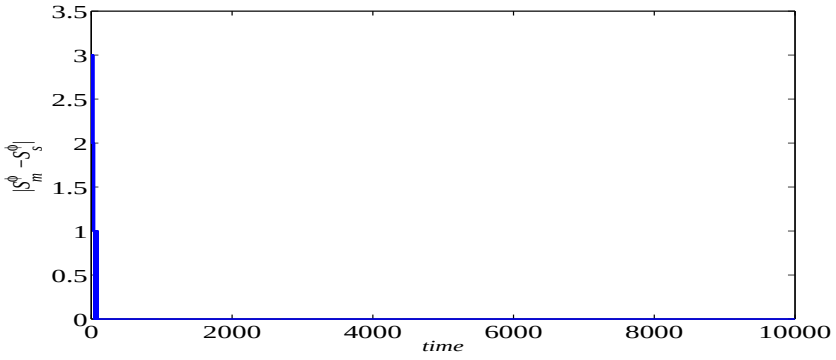

Figure 8: Difference between the itineraries of the master and the slave systems with initial condition: $\chi_{m0} = (4.8, 0.48, -0.29)^T$ for the master system and $\chi_{s01} = (1.01, 0.48, -0.29)^T$ for the slave system.

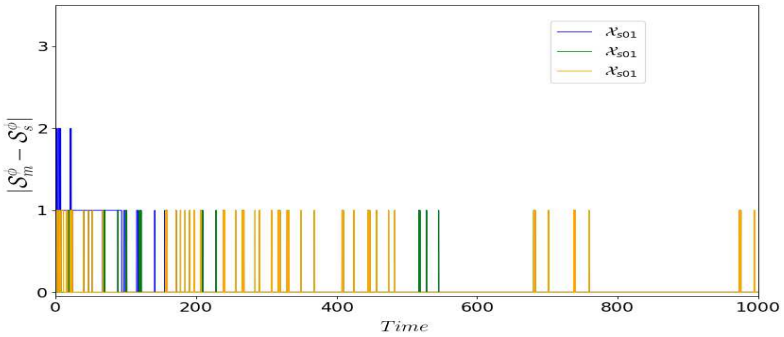

Figure 9: Difference between the itineraries of the master and the slave systems after relabeling the visited atoms for the initial conditions given in the example 4.3.

Master and slave systems, the inner linking matrix Γ and the coupling strength c play a crucial role to determining whether or not itinerary synchronization holds. For example, if we consider identical systems in the master-slave system given by (8) and (11) for the master and slave system, with inner linking matrix $\Gamma = \text{diag}\{0, 1, 0\}$, and $c = 10$, then itinerary synchronization holds, see Figure 8. It is worth noting that both systems are identical and oscillate presenting a triple-scroll attractor as shown in Figure 7 a). However, if the systems are quasi-symmetrical, the master-slave system given by (8), with (11), and (12) for the master and slave systems respectively, with the same inner linking matrix Γ, and strength coupling c given previously, itinerary synchronization is lost for certain recurrent periods of time. Figure (9) shows three signals which were generated by the difference between the master itinerary and slave itineraries after relabeling the atoms for different initial conditions for the slave system.

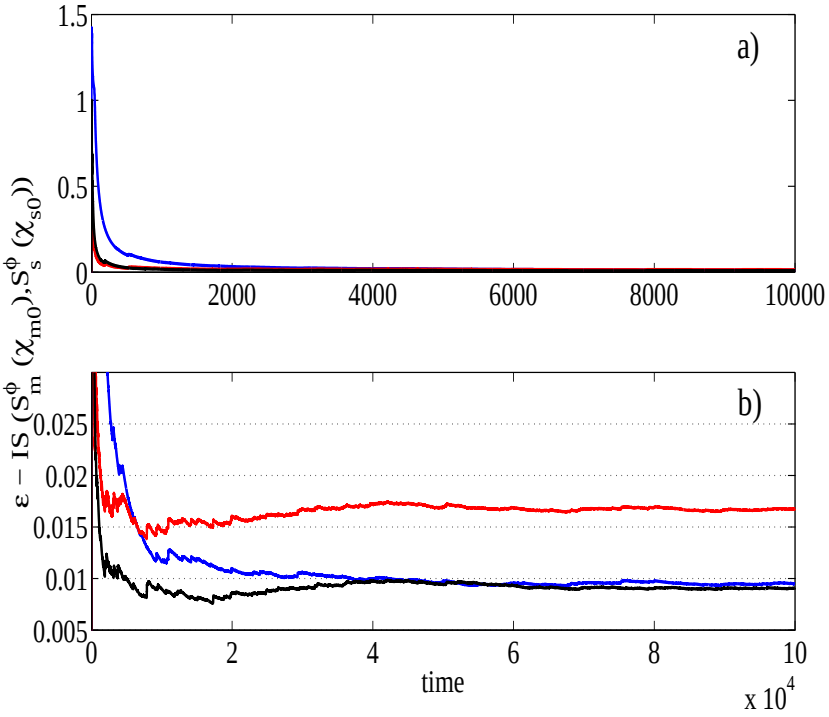

Figure 10: Computation of ϵ-Itinerary Synchronization between the master system and slave system after relabeling the visited atoms with the initial condition:$\chi_{m0} = (4.8, 0.48, -0.29)^T$ for the master system and $\chi_{s01} = (1.01, 0.48, -0.29)^T$ (blue line), $\chi_{s02} = (3.5, 0.48, -0.29)^T$ (red line), and $\chi_{s03} = (5.3, 0.48, -0.29)^T$ (black line) for the slave system, with coupling strength $c = 10$. For the time interval of arbitrary units a) $[0, 10^4]$; b) $[0, 10^5]$.

These small peaks along the error signals indicate that the master and slave systems go from one atom to other with an occasional time difference but master and slave systems are mostly itinerary synchronized, losing such synchrony only when a peaks occurs.

The concept of itinerary synchronization is strong for quasi-symmetrical systems. A weaker notion of itinerary synchronization is given as follows:

Definition 5.2. The master-slave system (8) is said to achieve ϵ-itinerary synchronization (ϵ-IS) if after relabeling the partition atoms

$$\limsup \frac{1}{t} \int_0^t |S_m^\phi(i, X_{m0} - S_s^\phi(i, X_{s0})| dt \leq \epsilon \tag{16}$$

for all initial conditions $\mathcal{X}_{m0}$ and $\mathcal{X}_{s0}$ in the basin of attraction.

The idea of ϵ-itinerary synchronization is that the systems are itinerary

synchronized except for infrequent (but persistent) time periods. The number ϵ quantifies the asymptotic frequency of asynchronous periods.

We investigate ϵ-itinerary synchronization of the master-slave system and it will be denoted by $\epsilon - IS(\mathcal{S}_m^{\phi}, \mathcal{S}_s^{\phi})$. Figure 10 a) shows the computation of ϵ-itinerary synchronization given by (16) when the strength coupling is $c = 10$ and the three initial conditions: χ_{s01} (blue line), χ_{s02} (red line) and χ_{s03} (black line), previously defined. The master-slave system demonstrates multistability and ϵ-itinerary synchronization for $\epsilon = 0.02$, see Figure 10 b).

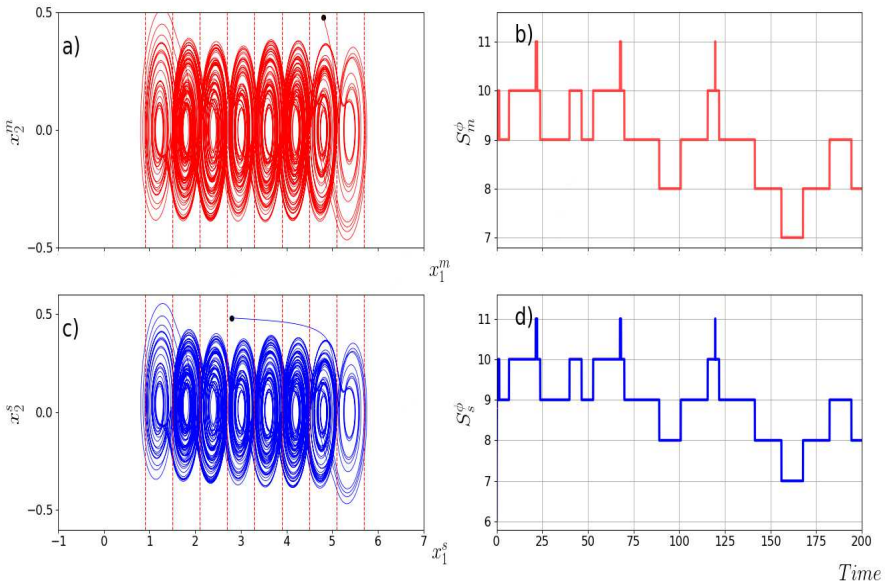

Figure 11: Projections of the master (red color) and slave (blue color) attractors onto the (x_1^m, x_2^m) plane and the (x_1^s, x_2^s) plane, respectively, with $\eta_m = 8$, $\eta_s = 3$, $\Gamma = \{1, 1, 1\}$, coupling strength $c = 10$; with initial conditions $\chi_{so} = (2.8, 0.48, -0.29)^T$ and $\chi_{mo} = (4.8, 0.48, -0.29)^T$ for the slave and master systems, respectively.

The multistability phenomenon is given by considering that the scroll degree of the master system is less that the scroll-degree of the slave system, and the inner linking matrix $\Gamma = \text{diag}\{0, 1, 0\}$. By changing the inner linking matrix to $\Gamma = \text{diag}\{1, 1, 1\}$ the multistability disappears and the slave system oscillates in the same atoms at the same time as the master system as shown in Figure 7 a). The inner linking matrix $\Gamma = \text{diag}\{1, 1, 1\}$ yields the scroll-degree determined by the master system in the slave system even if the scroll degree of the master system is greater than the scroll-degree of the slave system. For example, suppose that the master's scroll-degree is $\eta_m = 8$ and the slave's scroll-degree is $\eta_s = 3$. Now the signal for the master system is (12) and for the slave system is (11). We take the inner coupling matrix to be $\Gamma = \text{diag}\{1, 1, 1\}$ and the coupling strength to be $c = 10$. This inner coupling matrix Γ makes

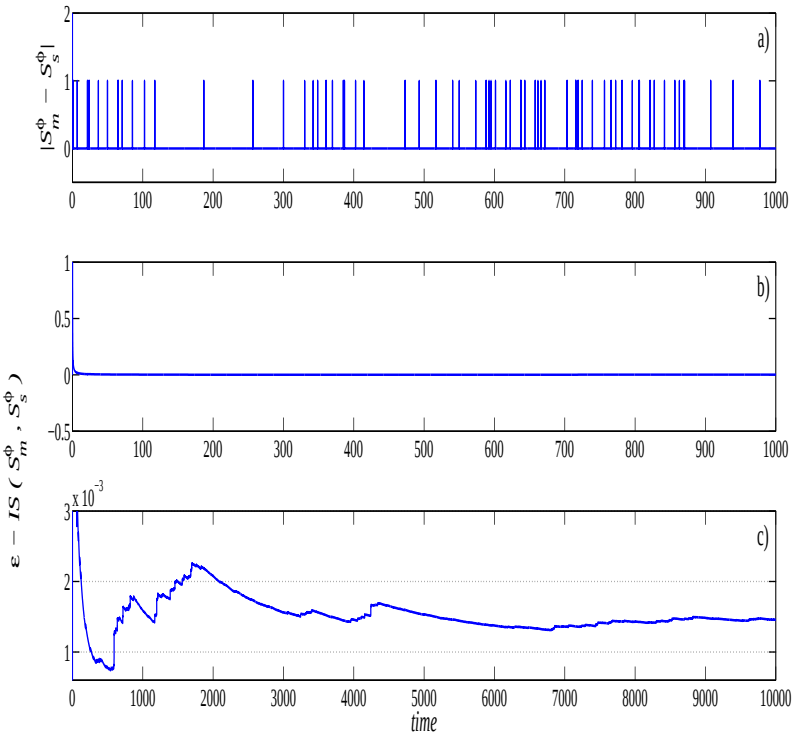

Figure 12: a) shows the difference between the itineraries of the master system and slave system, for $c = 10$ and $\Gamma = \text{diag}\{1, 1, 1\}$. b) and c) show the curve obtained by computing ϵ-itineraries of the master system and the slave system. For the time interval of arbitrary units b) $[0, 10^3]$; and c) $[0, 10^4]$.

$A - c\Gamma$ be Hurwitz for $0.2 < c$. Figures 11 a) and c) show the projections of the master and slave attractors given by (8) onto the (x_1^m, x_2^m) and (x_1^s, x_2^s) planes, respectively, generated with initial condition χ_{mo} given above for the master system and $\chi_{so} = (2.8, 0.48, -0.29)^T$ for the slave system. Note that the slave system increases its scroll-degree to $\eta_m = 8$. Figure 11 b) and d) shows the master and slave itineraries, respectively. Figure 12 a) shows the difference between the itineraries of the master system and slave system, for $c = 10$ and $\Gamma = \text{diag}\{1, 1, 1\}$, indicating that the master and slave systems present the same scroll degree because the offset of the signal is zero. Figure 12 b) shows the curve obtained by (16) which indicates ϵ-itinerary synchronization is achieved for $\epsilon = 0.003$, see Figure 12 c). In this setting the ϵ of ϵ-Itinerary Synchronization tends to zero as the coupling strength increases. This result is shown by the following proposition 5.3.

PROPOSITION (5.3). *Consider a master-slave system composed of quasi-symmetrical η-PWL systems described by* (8) *and signals $\kappa_m(\mathcal{X})$, and $\kappa_s(\mathcal{X})$ given by* (12) *and* (11)*, respectively, with $\Gamma = diag\{1,1,1\}$ and linear operator A given by* (6)*. As the coupling strength c tends to infinity then the master-slave system presents synchronization.*

Proof. The master slave system is given by

$$\begin{array}{ll} \dot{\mathcal{X}}_m & = A\mathcal{X}_m + B_{\kappa_m(\mathcal{X}_m)}, \\ \dot{\mathcal{X}}_s & = A\mathcal{X}_s + B_{\kappa_s(\mathcal{X}_s)} + c\Gamma(\mathcal{X}_m - \mathcal{X}_s). \end{array} \tag{17}$$

Defining the error between the master and slave systems as $e = \mathcal{X}_m - \mathcal{X}_s = (e_{x_1}, e_{x_2}, e_{x_3})^T$, where $e_{x_1} = x_{m1} - x_{s1}$, $e_{x_2} = x_{m2} - x_{s2}$ and $e_{x_3} = x_{m3} - x_{s3}$. Thus the error system is given by

$$\begin{array}{ll} \dot{e} & = Ae + B_{\kappa_m(\mathcal{X}_m)} - B_{\kappa_s(\mathcal{X}_s)} - c\Gamma e, \\ & = (A - c\Gamma)e + B_{\kappa_m(\mathcal{X}_m)} - B_{\kappa_s(\mathcal{X}_s)}, \\ & = \tilde{A}e + B_{\kappa_m(\mathcal{X}_m)} - B_{\kappa_s(\mathcal{X}_s)}, \end{array} \tag{18}$$

So the error system is given by

$$\begin{array}{ll} \dot{e}_{x_1} & = -ce_{x_1} + e_{x_2}, \\ \dot{e}_{x_2} & = -ce_{x_2} + e_{x_3}, \\ \dot{e}_{x_3} & = -\alpha_{31}e_{x_1} - \alpha_{32}e_{x_2} - (\alpha_{33} + c)e_{x_3} - (\beta_m - \beta_s), \end{array} \tag{19}$$

where β_m and β_s take values of the third entry of the vectors B_j, with $j = 3,4,5,6,7,8,9,10$ and B_j, with $j = 8,9,10$, respectively. Solving for the equilibrium point we find

$$e_{x_1} = (\beta_m - \beta_s)/(-\alpha_{31} - \alpha_{32} - (\alpha_{33} + c)c^2).$$

As $(\beta_m - \beta_s)$ is bounded e_{x_1} tends to zero when c tends to infinity. If e_{x_1} tends to zero then e_{x_2} and e_{x_3} also tend to zero. Therefore, the error system has $(0,0,0)^T$ as its sole equilibrium point. The master-slave system displays synchronization. □

In our numerical results we have considered only $c = 10$ and $\Gamma = \text{diag}\{0,1,0\}$ and $\Gamma = \text{diag}\{1,1,1\}$. But for sufficiently large values of c with both $\Gamma = \text{diag}\{0,1,0\}$ and $\Gamma = \text{diag}\{1,1,1\}$ the matrix $A - c\Gamma$ will have only eigenvalues with negative real part, which should lead to itinerary synchronization or ϵ-itinerary synchronization for small ϵ tending to 0 as the coupling strength increases (the presence of discontinuities in the PWL system makes difficult a rigorous rather than heuristic proof). For example if $\Gamma = \text{diag}\{1,1,1\}$ and c is greater than the positive real part of conjugate eigenvalues λ_2 and λ_3 of A then $A - c\Gamma$ with have all eigenvalues with negative real part.

6 Dynamical Networks

A dynamical network is composed of N coupled dynamical systems called nodes [20]. Each node is labeled by an index $i = 1, \ldots, N$ and described by a first ordinary differential equation system of the form $\dot{\mathcal{X}}_i(t) = f_i(\mathcal{X}_i(t))$, where $\mathcal{X}_i(t) = (x_{i1}(t), \ldots, x_{in}(t))^T \in \mathbb{R}^n$ is the state vector and, $f_i : \mathbb{R}^n \to \mathbb{R}^n$ is the vector field which describes the dynamical behavior of an i-th node when it is not connected to the network. We assume the coupling between neighboring nodes is linear so that the state equation of the entire network is described by the following equations:

$$\dot{\mathcal{X}}_i(t) = f_i(\mathcal{X}_i(t)) + c\sum_{j=1}^{N} \Delta_{ij}\Gamma(\mathcal{X}_j(t) - \mathcal{X}_i(t)), \quad i = 1, \ldots, N, \tag{20}$$

where c is the uniform coupling strength between the nodes and the inner linking matrix $\Gamma = \text{diag}\{r_1, \ldots, r_n\} \in \mathbb{R}^{n\times n}$ is described in (8). The matrix $\Delta = \{\Delta_{ij}\} \in \mathbb{R}^{N\times N}$ is called a coupling matrix if its elements are zero or one depending on which nodes are connected or not. Such a matrix contains the entire information about the network configuration topology. Specifically, if nodes are coupled with bidirectional links, then Δ is a symmetric matrix with the following entries: if there is a connection between node i and node j (with $i \neq j$), then $\Delta_{ij} = \Delta_{ji} = 1$; otherwise $\Delta_{ij} = \Delta_{ji} = 0$.

On the other hand, if the nodes are connected with unidirectional links, then Δ is a non-symmetric matrix with entries defined as follows: $\Delta_{ij} = 1$ (with $i \neq j$) if there is an edge directed from node j to node i; $\Delta_{ij} = 0$ if node j is not connected to node i.

Network (20) can be equivalently expressed in matrix form by using the Kronecker product as follows:

$$\dot{X}(t) = F(X(t)) + c(\Delta \otimes \Gamma)X(t),$$

where $X(t) = (\mathcal{X}_1, \ldots, \mathcal{X}_N)T \in \mathbb{R}^{Nn}$; $F(X(t)) = (f_1(\mathcal{X}_1), \ldots, f_N(\mathcal{X}_N))^T \in \mathbb{R}^{Nn}$; and $\otimes$ denotes the Kronecker product of matrices.

For the dynamical network (20) with a symmetric coupling matrix, one of the most studied collective phenomena is synchronization, which emerges when the dynamical behavior between nodes are correlated in-time (See [20] and references there in).

7 Ring and chain topology networks

We study the collective dynamics of N coupled quasi-symmetrical η-PWL systems which are connected by unidirectional links in a ring topology, *i.e.*, a network composed of an ensemble of master-slave systems coupled in a cascade configuration topology. In this context, a system defined in the node i is a slave system of a system defined in the node $i-1$, and also plays the role of a master system for a system defined in the node $i+1$. Figure 13 (a) shows a network

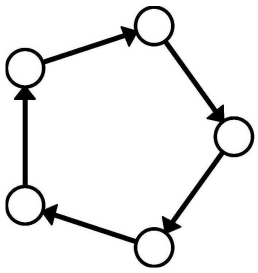

(a)

$$\Delta = \begin{pmatrix} 0 & 0 & 0 & 0 & 1 \\ 1 & 0 & 0 & 0 & 0 \\ 0 & 1 & 0 & 0 & 0 \\ 0 & 0 & 1 & 0 & 0 \\ 0 & 0 & 0 & 1 & 0 \end{pmatrix}$$

(b)

Figure 13: A network of $N = 5$ nodes coupled in a ring topology with unidirectional links. a) The network topology and b) the coupling matrix.

with a ring topology and 13 (b) its corresponding coupling matrix Δ. A network with such attributes is described by the following state equations:

$$\begin{cases} \dot{\mathcal{X}}_1 = A\mathcal{X}_1 + B_{\kappa_1(\mathcal{X}_1)} + c\Gamma(\mathcal{X}_N - \mathcal{X}_1), \\ \dot{\mathcal{X}}_2 = A\mathcal{X}_2 + B_{\kappa_2(\mathcal{X}_2)} + c\Gamma(\mathcal{X}_1 - \mathcal{X}_2), \\ \dot{\mathcal{X}}_3 = A\mathcal{X}_3 + B_{\kappa_3(\mathcal{X}_3)} + c\Gamma(\mathcal{X}_2 - \mathcal{X}_3), \\ \quad \vdots \qquad\qquad \vdots \\ \dot{\mathcal{X}}_N = A\mathcal{X}_N + B_{\kappa_N(\mathcal{X}_N)} + c\Gamma(\mathcal{X}_{N-1} - \mathcal{X}_N), \end{cases} \tag{21}$$

where $\mathcal{X}_i$, $i = 1, 2, \ldots, N$, denotes the state vector of each node. Notice that the system (21) is a dynamical network where each node differs only in the constant vector $B_{\kappa_i(\cdot)}$. In this context, we propose the following definition of a network of nearly identical nodes:

Definition 7.1. A network of nearly identical nodes is a network composed of nodes with dynamics given by quasi-symmetrical η-PWL systems, *i.e.*, $A_i = A_j = A$, $\eta_i \neq \eta_j$ and $\kappa_i(\cdot) \neq \kappa_j(\cdot)$ $\forall i, j = 1, 2, \ldots, N$ whose state equation is written as follows:

$$\dot{\mathcal{X}}_i = A\mathcal{X}_i + B_{\kappa_i(\mathcal{X}_i)} + c\sum_{j=1}^{N} \Delta_{ij}\Gamma(\mathcal{X}_j - \mathcal{X}_i), \quad i = 1, \ldots, N. \tag{22}$$

Note that (22) corresponds to a dynamical network with a configuration topology given by the coupling matrix $\Delta = \{\Delta_{ij}\} \in \mathbb{R}^{N\times N}$. In particular, for a ring topology (Figure 13), the equation (22) becomes the equation (21).

We first study the collective behavior of a nearly identical network (22) assuming that the coupling matrix corresponds to a network with a ring topology and with unidirectional links. We are interested in knowing what is the scroll-degree of all the nodes in this kind of network with different scroll-degree in its nodes and when none of them is the leading node (master system). In Section 5,

a master system forces the slave system to have the same scroll degree and the master-slave system achieves ϵ-Itinerary Synchronization. However in a ring topology network each node behaves as the master system of the following node but at the same time it behaves as a slave system of the preceding node. Finally we consider the case in which the network (22) has a directed chain topology where the leading node has the maximum or the minimum scroll-degree.

7.1 Node's dynamics

In this section we consider the switching regions as in Definition 2.1. The dynamics of the i-node is controlled by the (i-1)-node, see equation (21).

Since the dynamics of a single node is governed by an UDS system plus a coupling signal which comes from only one node of the network, we know that the linear operator is diagonalizable *i.e.* exist a matrix $Q \in \mathbb{R}^{3\times 3}$ such that $\Lambda = Q^{-1}AQ$ with $\Lambda = \text{diag}[\lambda_1, \lambda_2, \lambda_3]$. So the node's dynamics is given by

$$\begin{array}{ll} \dot{x}_{i1} & = -cx_{i1} + x_{i2} + cx_{(i-1)1}, \\ \dot{x}_{i2} & = -cx_{i2} + x_{i3} + cx_{(i-1)2}, \\ \dot{x}_{i3} & = -1.5x_{i1} - x_{i2} - (1+c)x_{i3} + \beta_3^{\kappa i} + cx_{(i-1)3}, \end{array} \tag{23}$$

where $\mathcal{X}_i = (x_{i1}, x_{i2}, x_{i3})^T$, for $i = 1, \ldots, N$ and consider that if $n = 1$ then $n - 1 = N$. $\beta_3^{\kappa i} \in \Delta_\beta = \{0, 0.9, 1.8, 2.7, 3.6, 4.5, 5.4, 6.3, , 7.2, 8.1\}$ is determined by the third component of constant vectors $B_{\kappa i} = (0, 0, \beta_3^{\kappa i})$. By introducing a change of variable $z_i = (z_1^i, z_2^i, z_3^i)^T = (x_{i1} - k_1, x_{i2} - k_2, x_{i3} - k_3)^T$ each the trajectory $\mathcal{X}_i(t)$ goes to an atom P_i of the partition $\mathcal{P}$, with $k_1 = \beta_3^{\kappa i}/(1.5 + c + c^2 + c^3)$, $k_2 = cK_1$, and $k_3 = c^2 k_1$. We rewrite the equation (23) as follows:

$$\begin{array}{ll} \dot{z}_1^i & = -cz_1^i + z_2^i + f_1, \\ \dot{z}_2^i & = -cz_2^i + z_3^i + f_2, \\ \dot{z}_3^i & = -1.5z_1^i - z_2^i - (1+c)z_3^i + f_3, \end{array} \tag{24}$$

where $f_1 = cx_{(i-1)1}$, $f_2 = cx_{(i-1)2}$, and $f_3 = cx_{(i-1)3}$ are external signal of the i-node that come from $(i-1)$-node. So the system (24) is given as follows:

$$\dot{z}_i = A_c z_i + F^{i-1}, \quad i = 1, \ldots, N, \tag{25}$$

where $A_c = A + \text{diag}[-c, -c, -c]$ and $F^{i-1} = [f_1, f_2, f_3]^T$ is conformed from the state vector of the $(i-1)$-node. If $c > 0.1020$ then A_c is Hurwitz. For the particular value of $c = 10$ the eigenvalues are: $\lambda_{c1} = -11.2041$, $\lambda_{c2} = -9.8980 + 1.1115i$, $\lambda_{c3} = -9.8980 - 1.1115i$. The solution of the nonhomogeneous linear system (25) is:

$$z_i(t) = e^{A_c t} z_i(0) + e^{A_c t} \int_0^t e^{-A_c \tau} F(\tau) d\tau, \tag{26}$$

where $z_i(0)$ is the initial condition of the i-th node in the new state variable. The first term of the right hand side of the equation (26) converges to zero when

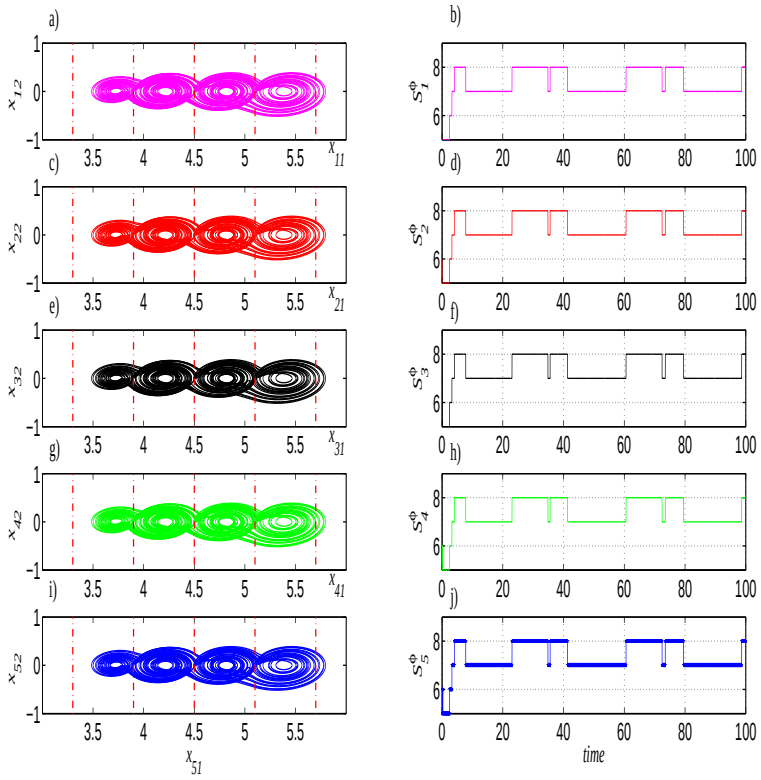

Figure 14: Dynamics of a nearly identical network (22) with coupling strength $c = 10$ and $\Gamma = \text{diag}\{1, 1, 1\}$; the scroll-degree and initial condition for each node are given in Table (1): a); c); e); g); i); The projections of the attractors onto the plane (x_{i1}, x_{i2}) of the node 1,2,3,4 and 5 respectively (Transient were removed); and b); d); f); h); j) its itinerary.

$t \to \infty$. So the node's dynamics is given as follows

$$\mathcal{X}_i(t) = (k_1, k_2, k_3)^T + e^{A_c t} \int_0^t e^{-A_c \tau} \mathcal{X}_{i-1}(\tau) d\tau. \tag{27}$$

The dynamics of $i-$node is determined by the $(i-1)$-node, so the collective dynamics of N coupled quasi-symmetrical η-PWL systems which are connected by unidirectional links in a ring topology can present synchronous behavior if the different node states commute from one atom P_i to other P_j presenting the same constant vector $(k_1, k_2, k_3)^T$.

7.2 Dynamics in a ring topology

We consider a ring network with five nodes, *i.e.*, $N = 5$ nearly identical nodes described in (22) and coupled in a ring topology. We assume that each node's dynamic is described by the same linear operator A (*i.e* they are quasi-symmetrical) and a subset of the set of constant vectors $\mathbf{B} = \{B_1, B_2, \ldots, B_{10}\}$ which are those given by (6). Further, for each node we select the scroll-degree (η_i) and its corresponding initial condition according to Table (1).

Node's label	Scroll-degree	Initial condition
1	10	$(0.227, -0.216, -0.359)^T$
2	5	$(3.014, -0.371, -0.271)^T$
3	3	$(5.349, -0.424, -0.279)^T$
4	8	$(1.402, -0.205, -0.316)^T$
5	6	$(2.452, -0.266, -0.308)^T$

Table 1: The scroll-degree (η_i) and its corresponding initial condition for each node in the nearly identical network coupled in a ring topology for Examples 7.2 and 7.3.

The signal for the first node with scroll-degree $\eta_1 = 10$ is given by (7) where is defined the partition $\mathcal{P} = \{P_1, \ldots, P_{10}\}$; for the third and fourth nodes with scroll-degree $\eta_3 = 3$ and partition $\mathcal{P} = \{P_8, \ldots, P_{10}\}$; and $\eta_4 = 8$ and partition $\mathcal{P} = \{P_3, \ldots, P_{10}\}$ are given by (11) and (12) respectively. For the second node with scroll degree $\eta_2 = 5$ the switching signal is given as follows:

$$\kappa_5(\mathcal{X}) = \begin{cases} 1, & \text{if} \quad \mathcal{X} \in P_{10} = \{\mathcal{X} \in \mathbb{R}^3 : x_1 \geq 5.1\}; \\ 2, & \text{if} \quad \mathcal{X} \in P_9 = \{\mathcal{X} \in \mathbb{R}^3 : 4.5 \leq x_1 < 5.1\}; \\ 3, & \text{if} \quad \mathcal{X} \in P_8 = \{\mathcal{X} \in \mathbb{R}^3 : 3.9 \leq x_1 < 4.5\}; \\ 4, & \text{if} \quad \mathcal{X} \in P_7 = \{\mathcal{X} \in \mathbb{R}^3 : 3.3 \leq x_1 < 3.9\}; \\ 5, & \text{if} \quad \mathcal{X} \in P_6 = \{\mathcal{X} \in \mathbb{R}^3 : x_1 < 3.3\}. \end{cases} \tag{28}$$

And for the fifth node with scroll degree $\eta_5 = 6$ is

$$\kappa_6(\mathcal{X}) = \begin{cases} 1, & \text{if} \quad \mathcal{X} \in P_{10} = \{\mathcal{X} \in \mathbb{R}^3 : x_1 \geq 5.1\}; \\ 2, & \text{if} \quad \mathcal{X} \in P_9 = \{\mathcal{X} \in \mathbb{R}^3 : 4.5 \leq x_1 < 5.1\}; \\ 3, & \text{if} \quad \mathcal{X} \in P_8 = \{\mathcal{X} \in \mathbb{R}^3 : 3.9 \leq x_1 < 4.5\}; \\ 4, & \text{if} \quad \mathcal{X} \in P_7 = \{\mathcal{X} \in \mathbb{R}^3 : 3.3 \leq x_1 < 3.9\}; \\ 5, & \text{if} \quad \mathcal{X} \in P_6 = \{\mathcal{X} \in \mathbb{R}^3 : 2.7 \leq x_1 < 3.3\}; \\ 6, & \text{if} \quad \mathcal{X} \in P_5 = \{\mathcal{X} \in \mathbb{R}^3 : x_1 < 2.7\}. \end{cases} \tag{29}$$

The scroll-degree is determined numerically under two inner coupling matrices: $\Gamma = \text{diag}\{1, 1, 1\}$ and $\Gamma = \text{diag}\{1, 0, 0\}$, and the ring topology network with five nodes.

Example 7.2. For the nearly identical network described above, we assume that the coupling strength is $c = 10$, the inner coupling matrix is $\Gamma = \text{diag}\{1, 1, 1\}$. We solve numerically the nearly identical network (22) with the scroll-degree

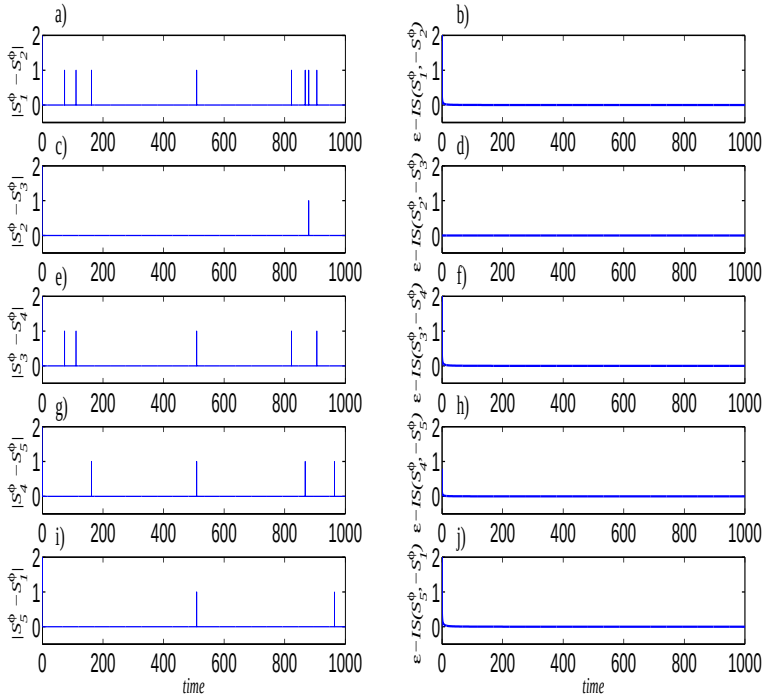

Figure 15: Difference between the itineraries of the nodes of a nearly identical network (22) with coupling strength $c = 10$ and $\Gamma = \text{diag}\{1, 1, 1\}$; the scroll-degree and initial condition for each node are given in Table (1). a) $|\mathcal{S}_1^\phi - \mathcal{S}_2^\phi|$; c) $|\mathcal{S}_2^\phi - \mathcal{S}_3^\phi|$; e) $|\mathcal{S}_3^\phi - \mathcal{S}_4^\phi|$; g) $|\mathcal{S}_4^\phi - \mathcal{S}_5^\phi|$; i)$|\mathcal{S}_5^\phi - \mathcal{S}_1^\phi|$; and b)$\epsilon - IS(\mathcal{S}_1^\phi, \mathcal{S}_2^\phi)$; d) $\epsilon - IS(\mathcal{S}_{s2}^\phi, \mathcal{S}_3^\phi)$; f) $\epsilon - IS(\mathcal{S}_3^\phi, \mathcal{S}_4^\phi)$; h) $\epsilon - IS(\mathcal{S}_4^\phi, \mathcal{S}_5^\phi)$; j) $\epsilon - IS(\mathcal{S}_5^\phi, \mathcal{S}_1^\phi)$.

and initial condition given in Table (1) and using a Runge-Kutta method with 10,000,000 time iterations and step size $h = 0.01$.

In the first column of the Figure 14 we show the projections of the attractors onto the planes (x_{i1}, x_{i2}) after transients, with $i = 1, \ldots, 5$, note that independently of the initial conditions, the trajectories of all nodes converge to an attractor with four scrolls and one of them is a smaller scroll than the others (the left scroll). If we count this smaller scroll, then the ring topology network displays a $\eta = 4$ scroll degree. In the right column of the Figure 14, we display its corresponding itinerary in a short interval of time in order to appreciate the time elapsed that the trajectory of each node spends in a given atom. We can see that in this short time the itineraries behave identically and definition of itinerary synchronization is fulfilled. However if we analyze the difference between itineraries of the $(i-1)-th$ node and $i-th$ node in a longer period of time it is possible to see that the nodes are briefly out of itinerary synchronization. For example, Figure 15 a) shows the difference of itineraries of the first node

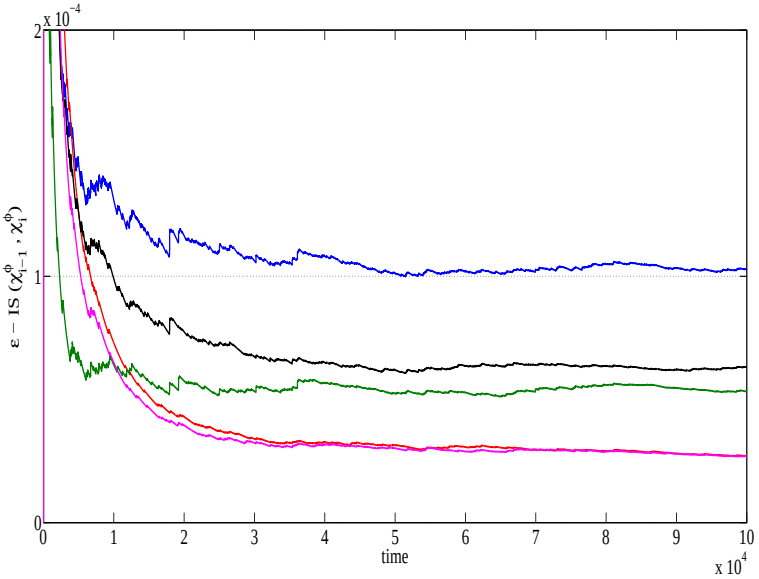

Figure 16: Different curves computed by (16) for ϵ-itinerary synchronization between the nodes of a nearly identical network (22) with coupling strength $c = 10$ and $\Gamma = \text{diag}\{1, 1, 1\}$; the scroll-degree and initial condition for each node are given in Table (1): blue line for $\epsilon - IS(\mathcal{S}_1^\phi, \mathcal{S}_2^\phi)$; red line for $\epsilon - IS(\mathcal{S}_{s2}^\phi, \mathcal{S}_3^\phi)$; black line for $\epsilon - IS(\mathcal{S}_3^\phi, \mathcal{S}_4^\phi)$; green line for $\epsilon - IS(\mathcal{S}_4^\phi, \mathcal{S}_5^\phi)$; and magenta line for $\epsilon - IS(\mathcal{S}_5^\phi, \mathcal{S}_1^\phi)$.

and the second node $|\mathcal{S}_1^\phi - \mathcal{S}_2^\phi|$, remember that the coupling is unidirectional, *i.e.*, the first node acts as a master system on the second node which acts as a slave system. These two nodes are synchronized when the difference between itineraries is zero and out of synchronization otherwise. Figure 15 shows the difference of itineraries of: c) the second node and the third node $|\mathcal{S}_2^\phi - \mathcal{S}_3^\phi|$; e) the third node and the fourth node $|\mathcal{S}_3^\phi - \mathcal{S}_4^\phi|$; g) the fourth node and the fifth node $|\mathcal{S}_4^\phi - \mathcal{S}_5^\phi|$; and i) the fifth node and the first node $|\mathcal{S}_5^\phi - \mathcal{S}_1^\phi|$. Figure 15 b) shows the ϵ-itinerary synchronization between the first node and the second node, it is possible to see that ϵ-itinerary synchronization definition is fulfilled. Figures 15 d), f), h, and j) show the ϵ-itinerary synchronizations between the $i-th$ node and its $(i+1)-th$ node: d) $\epsilon - IS(\mathcal{S}_2^\phi, \mathcal{S}_3^\phi)$; f) $\epsilon - IS(\mathcal{S}_3^\phi, \mathcal{S}_4^\phi)$; h) $\epsilon - IS(\mathcal{S}_4^\phi, \mathcal{S}_5^\phi)$; j) $\epsilon - IS(\mathcal{S}_5^\phi, \mathcal{S}_1^\phi)$. In conclusion, all the nodes of the ring topology network present ϵ-itinerary synchronization by considering $\epsilon = 0.0002$, see Figure 16. This Figure shows the different curves computed by (16) for ϵ-itinerary synchronization between the nodes of a nearly identical network (22) with coupling strength $c = 10$ and $\Gamma = \text{diag}\{1, 1, 1\}$; the scroll-degree and initial condition for each node are given in Table (1): blue line for $\epsilon - IS(\mathcal{S}_1^\phi, \mathcal{S}_2^\phi)$; red line for $\epsilon - IS(\mathcal{S}_{s2}^\phi, \mathcal{S}_3^\phi)$; black line for $\epsilon - IS(\mathcal{S}_3^\phi, \mathcal{S}_4^\phi)$; green line for $\epsilon - IS(\mathcal{S}_4^\phi, \mathcal{S}_5^\phi)$; and magenta line for $\epsilon - IS(\mathcal{S}_5^\phi, \mathcal{S}_1^\phi)$.

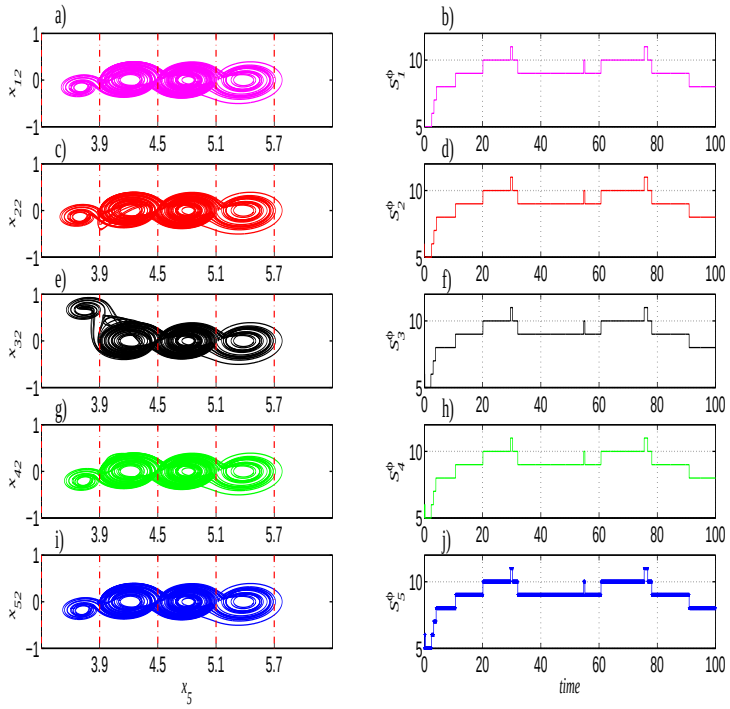

Figure 17: Dynamics of a nearly identical network (22) with coupling strength $c = 10$ and $\Gamma = \text{diag}\{1, 0, 0\}$; the scroll-degree and initial condition for each node are given in Table (1): a); c); e); g); i); The projections of the attractors onto the plane (x_1, x_2) of the node 1,2,3,4 and 5 respectively (Transients were removed); and b); d); f); h); j) its itinerary.

Example 7.3. The dynamics of the network composed of N quasi-symmetrical η-PWL systems described above can display several behaviors depending on the inner coupling matrix Γ. The collective dynamics is affected when we suppress some variable state in the inner connection. For example, in the first column of Figure 17 when we suppress two state variables from the inner coupling matrix $\Gamma = \text{diag}\{1, 0, 0\}$, a deformation of the scroll attractor is achieved specially over the node with the smallest node-degree (in this case, for the node with scroll-degree 3). In the first column of the Figure 17 we show the projections of the attractors onto the planes (x_{i1}, x_{i2}), with $i = 1, \ldots, 5$, the ring topology network displays a $\eta = 4$ scroll degree. In the right column of the Figure 17, we display its corresponding itinerary in a short interval of time in order to appreciate the time elapsed that the trajectory of each node spends in a given atom. We can see that in this short time the itineraries behave identically and definition of itinerary synchronization is fulfilled again that for $\Gamma = \text{diag}\{1, 1, 1\}$. And the difference between itineraries of the $(i-1) - th$ node and $i - th$ node is shown

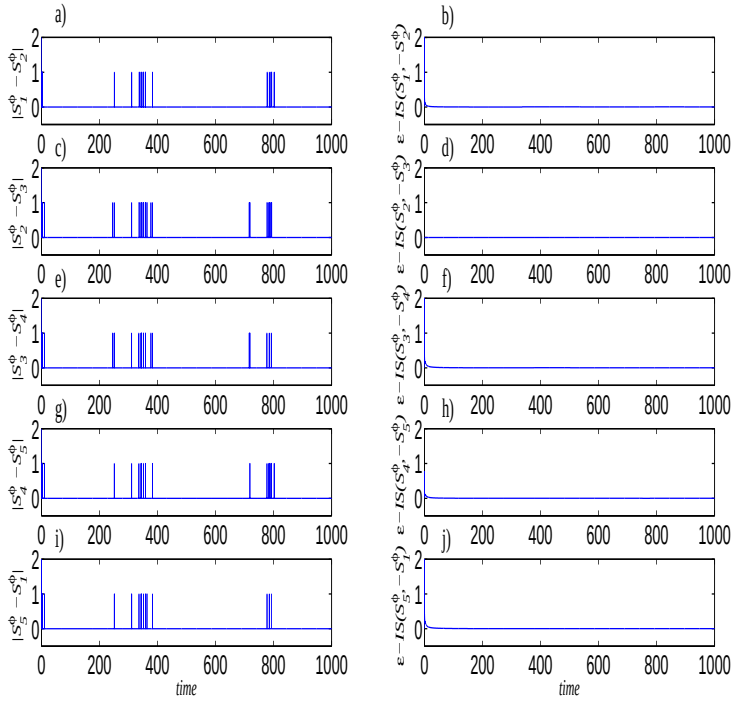

Figure 18: Difference between the itineraries of the nodes of a nearly identical network (22) with coupling strength $c = 10$ and $\Gamma = \text{diag}\{1, 0, 0\}$; the scroll-degree and initial condition for each node are given in Table (1). a) $|\mathcal{S}_1^\phi - \mathcal{S}_2^\phi|$; c) $|\mathcal{S}_2^\phi - \mathcal{S}_3^\phi|$; e) $|\mathcal{S}_3^\phi - \mathcal{S}_4^\phi|$; g) $|\mathcal{S}_4^\phi - \mathcal{S}_5^\phi|$; i)$|\mathcal{S}_5^\phi - \mathcal{S}_1^\phi|$; and b)$\epsilon - IS(\mathcal{S}_1^\phi, \mathcal{S}_2^\phi)$; d) $\epsilon - IS(\mathcal{S}_2^\phi, \mathcal{S}_3^\phi)$; f) $\epsilon - IS(\mathcal{S}_3^\phi, \mathcal{S}_4^\phi)$; h) $\epsilon - IS(\mathcal{S}_4^\phi, \mathcal{S}_5^\phi)$; j) $\epsilon - IS(\mathcal{S}_5^\phi, \mathcal{S}_1^\phi)$.

in Figure 18: a) $|\mathcal{S}_1^\phi - \mathcal{S}_2^\phi|$; c) $|\mathcal{S}_2^\phi - \mathcal{S}_3^\phi|$; e) $|\mathcal{S}_3^\phi - \mathcal{S}_4^\phi|$; g) $|\mathcal{S}_4^\phi - \mathcal{S}_5^\phi|$; and i) $|\mathcal{S}_5^\phi - \mathcal{S}_1^\phi|$. The second column of Figure 18 shows the ϵ- itinerary synchronizations between the $i-th$ node and the $(i-1)-th$ node: b) $\epsilon - IS(\mathcal{S}_1^\phi, \mathcal{S}_2^\phi)$; d) $\epsilon - IS(\mathcal{S}_2^\phi, \mathcal{S}_3^\phi)$; f) $\epsilon - IS(\mathcal{S}_3^\phi, \mathcal{S}_4^\phi)$; h) $\epsilon - IS(\mathcal{S}_4^\phi, \mathcal{S}_5^\phi)$; and j) $\epsilon - IS(\mathcal{S}_5^\phi, \mathcal{S}_1^\phi)$. In conclusion, in this example all the nodes of the ring topology network are fulfilled the definition of ϵ-itinerary synchronization by considering $\epsilon = 0.02$, see Figure 19. This Figure shows the different curves computed by (16) for ϵ-itinerary synchronization between the nodes of a nearly identical network (22) with coupling strength $c = 10$ and $\Gamma = \text{diag}\{1, 0, 0\}$; the scroll-degree and initial condition for each node are given in Table (1): blue line for $\epsilon - IS(\mathcal{S}_1^\phi, \mathcal{S}_2^\phi)$; red line for $\epsilon - IS(\mathcal{S}_{s2}^\phi, \mathcal{S}_3^\phi)$; black line for $\epsilon - IS(\mathcal{S}_3^\phi, \mathcal{S}_4^\phi)$; green line for $\epsilon - IS(\mathcal{S}_4^\phi, \mathcal{S}_5^\phi)$; and magenta line for $\epsilon - IS(\mathcal{S}_5^\phi, \mathcal{S}_1^\phi)$. However they do not satisfy the definition of complete synchronization due to the third node are oscillating in a different manner, see Figure 17 e).

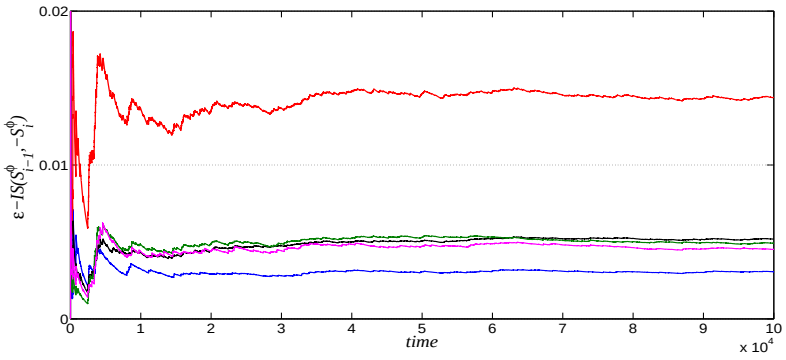

Figure 19: Different curves computed by (16) for ϵ-itinerary synchronization between the nodes of a nearly identical network (22) with coupling strength $c = 10$ and $\Gamma = \text{diag}\{1, 0, 0\}$; the scroll-degree and initial condition for each node are given in Table (1): blue line for $\epsilon - IS(\mathcal{S}_1^\phi, \mathcal{S}_2^\phi)$; red line for $\epsilon - IS(\mathcal{S}_{s2}^\phi, \mathcal{S}_3^\phi)$; black line for $\epsilon - IS(\mathcal{S}_3^\phi, \mathcal{S}_4^\phi)$; green line for $\epsilon - IS(\mathcal{S}_4^\phi, \mathcal{S}_5^\phi)$; and magenta line for $\epsilon - IS(\mathcal{S}_5^\phi, \mathcal{S}_1^\phi)$.

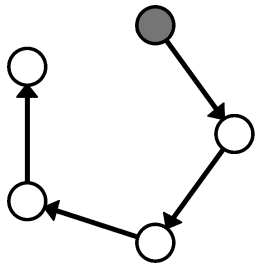

(a)

$$\Delta = \begin{pmatrix} 0 & 0 & 0 & 0 & 0 \\ 1 & 0 & 0 & 0 & 0 \\ 0 & 1 & 0 & 0 & 0 \\ 0 & 0 & 1 & 0 & 0 \\ 0 & 0 & 0 & 1 & 0 \end{pmatrix}$$

(b)

Figure 20: A network of $N = 5$ nodes coupled in a open ring topology with directional links. (a) The network topology and (b) the coupling matrix.

7.3 Dynamics in a directed chain topology

In this subsection we present numerical results for the case in which the network has a directed chain topology. This change transforms the network topology from a ring configuration to a chain (open ring) configuration as we illustrate in Figure 20; where we also show the corresponding coupling matrix that describes this network.

After removing a node, the black node in Figure 20 (a), which we call the leader node, plays the role of the master system for the rest of the nodes. The second node is the slave system for the leader node, but it is also the master system for the third node, and so on. The idea is to explore if such a leader node governs or not the collective dynamics of the rest of the nodes. In this work we assume that the scroll-degree of the master node corresponds to the largest or the smallest scroll-degree. Specifically we consider two examples: the

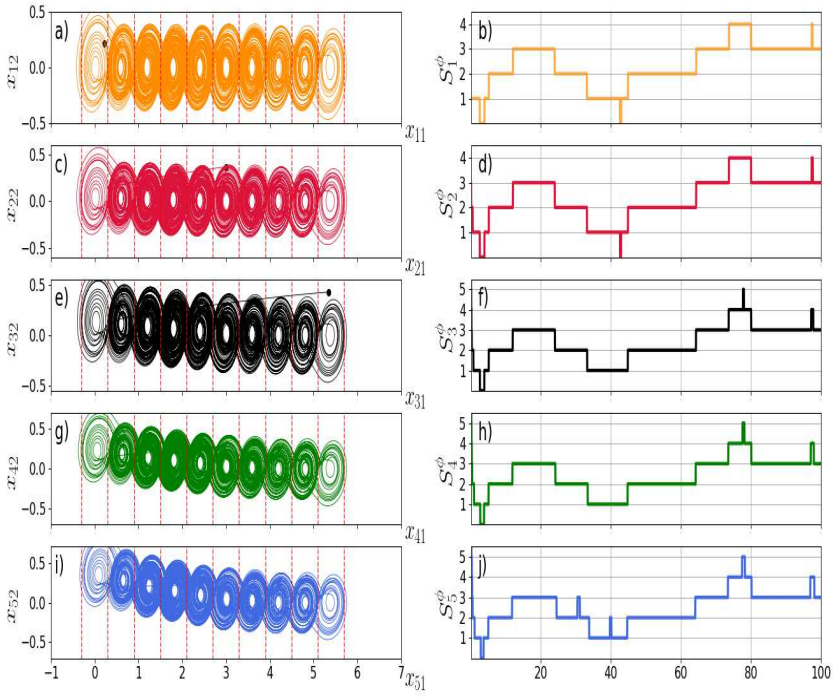

Figure 21: a), c), e), g), i): the projections of the attractors onto the plane (x_{i1}, x_{i2}), with $i = 1, \ldots, 5$, of the nodes of a nearly identical network (22) in an directed chain topology with coupling strength $c = 10$, $\Gamma = \text{diag}\{1, 1, 1\}$ and where the first node has scroll-degree $\eta_i = 10$. b), d), f), h), j): the itinerary of each node.

first node has scroll-degree ten or three.

7.3.1 Master system with maximum scroll-degree

Figure 21 shows the projections onto the plane (x_{i1}, x_{i2}), with $i = 1, \ldots, 5$, of the attractors generated in each node by the nearly identical network (22) with a chain configuration. For this example we assume that the first node has scroll-degree $\eta_1 = 10$, and the nodes are connected with coupling strength $c = 10$ and inner coupling matrix $\Gamma = \text{diag}\{1, 1, 1\}$. The node's scroll-degree and its corresponding initial condition are given in Table (1). All the nodes imitate the dynamics of the master system and change their dynamics to attain the same scroll-degree. In this context, the scroll-degree of the leader node dominates and itinerary synchronization is achieved in short periods of time as is shown in the second column of Figure 21. However for a long period of time it is possible to observe spikes and all the nodes of the network present ϵ- Itinerary Synchronization for $\epsilon = 0.02$, see Figure 22 a). This figure 22 a) shows the

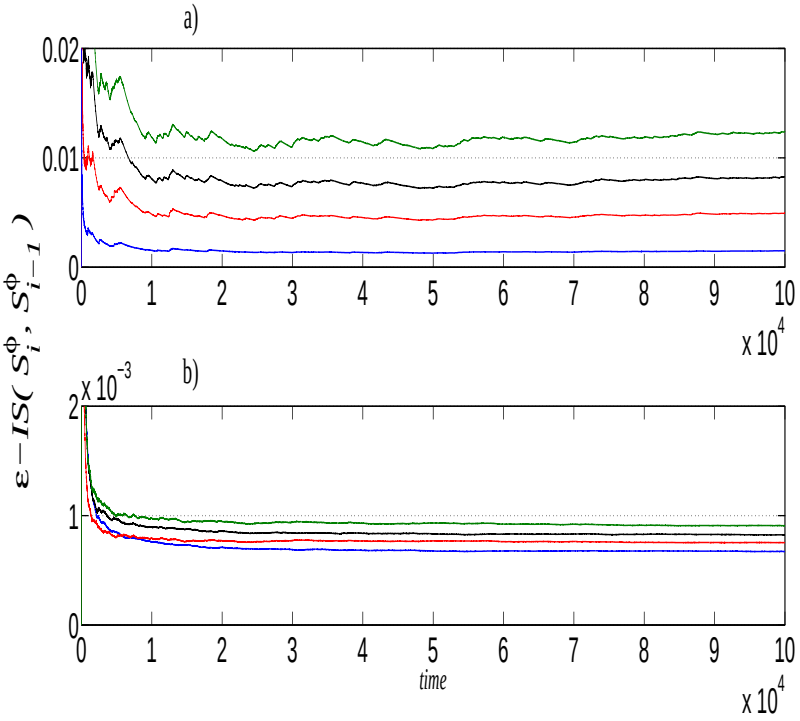

Figure 22: Different curves computed by (16) for ϵ-itinerary synchronization between the nodes of a nearly identical network (22) in an directed chain topology with coupling strength $c = 10$ and $\Gamma = \text{diag}\{1, 1, 1\}$; the scroll-degree and initial condition for each node are given in Table (1): blue line for $\epsilon - IS(\mathcal{S}_1^\phi, \mathcal{S}_2^\phi)$; red line for $\epsilon - IS(\mathcal{S}_2^\phi, \mathcal{S}_3^\phi)$; black line for $\epsilon - IS(\mathcal{S}_3^\phi, \mathcal{S}_4^\phi)$; and green line for $\epsilon - IS(\mathcal{S}_4^\phi, \mathcal{S}_5^\phi)$. a) Master system with maximum scroll-degree, and b) Master system with minimum scroll-degree.

different curves computed by (16) for ϵ- itinerary synchronization between the nodes of a nearly identical network (22): blue line for $\epsilon - IS(\mathcal{S}_1^\phi, \mathcal{S}_2^\phi)$; red line for $\epsilon - IS(\mathcal{S}_2^\phi, \mathcal{S}_3^\phi)$; black line for $\epsilon - IS(\mathcal{S}_3^\phi, \mathcal{S}_4^\phi)$; and green line for $\epsilon - IS(\mathcal{S}_4^\phi, \mathcal{S}_5^\phi)$.

7.3.2 Master system with minimum scroll-degree

Now we assume that after removing the link, the first node has scroll-degree $\eta_1 = 3$, and the rest of the nodes have the scroll-degree and initial condition given in Table (1). As before, we select a coupling strength $c = 10$ and $\Gamma = \text{diag}\{1, 1, 1\}$. In Figure 23 we observe that all the nodes reduce their scroll-degree to three *i.e.* the nodes adopt the scroll-degree of the first node, in this case Figure 23 e) shows the leader node. Furthermore, the rest of the nodes achieve ϵ-Itinerary Synchronization for the set of given initial conditions and $\epsilon = 0.001$, see Figure 22 b). This figure 22 b) shows the different curves

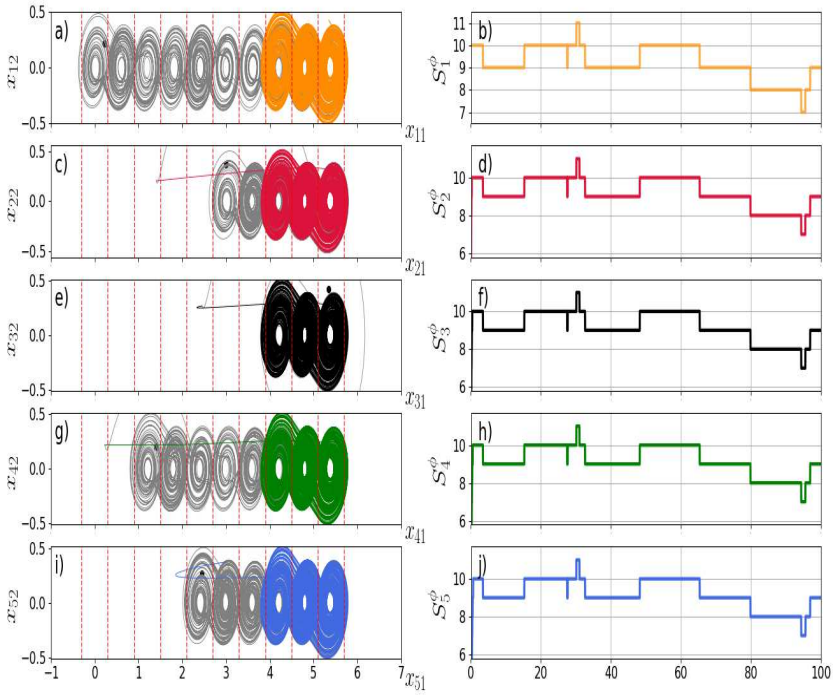

Figure 23: a), c), e), g), i): The projections of the attractors onto the plane (x_{i1}, x_{i2}), with $i = 1, \ldots, 5$, of a nearly identical network (22) in a directed chain topology with coupling strength $c = 10$, $\Gamma = \text{diag}\{1, 1, 1\}$ and where the first node has scroll-degree $\eta_i = 3$. b), d), f), h), j): The itinerary of each node.

computed by (16) for ϵ- itinerary synchronization between the nodes of a nearly identical network (22): blue line for $\epsilon - IS(\mathcal{S}_1^\phi, \mathcal{S}_2^\phi)$; red line for $\epsilon - IS(\mathcal{S}_2^\phi, \mathcal{S}_3^\phi)$; black line for $\epsilon - IS(\mathcal{S}_3^\phi, \mathcal{S}_4^\phi)$; and green line for $\epsilon - IS(\mathcal{S}_4^\phi, \mathcal{S}_5^\phi)$.

8 Conclusions

We have considered PWL systems, generated via heteroclinic orbits and whose dynamics exhibits a double scroll attractor. The concept of scroll-degree has been introduced to describe the number of scrolls that the PWL system displays in its attractor. We study the dynamics of this PWL system by symbolic dynamics, given by a natural partition of the state space. Synchronization phenomena has been studied in a master-slave system using two inner linking matrices: $\Gamma = \text{diag}\{0, 1, 0\}$ and $\Gamma = \text{diag}\{1,\ 1, 1\}$. For both inner linking matrices and the coupling strength $c = 10$ we found that the master-slave system presents itinerary synchronization when the systems are identical, and for

$\Gamma = \text{diag}\{0, 1, 0\}$ and the same coupling strength then the master-slave system presents ϵ-itinerary synchronization when the systems are quasi-symmetrical. This leads to multistability behavior if the scroll-degree of the master system is less than the slave system.

Our numerical results show that for sufficiently large coupling strength, ϵ-itinerary synchronization for small ϵ is achieved for different configurations of the inner coupling matrix. Furthermore, we observe in the multistability regimen that if the scroll-degree of the master system is less than the slave degree, then the slave system reduces its scroll-degree and, depending on its initial condition, it evolves between distinct basins of attractions. On the hand, if the scroll-degree of the master system is greater than the slave, we observe that the slave system increase its scroll-degree to be the same as the master, and ϵ-itinerary synchronization is also achieved.

The concept of network of nearly identical nodes was introduced to characterize a dynamical network composed of PWL systems with different scroll degrees. We investigated the collective dynamics of an N-coupled PWL-systems with different scroll-degree and connected in a master-slave scheme, that is, a unidirectional ring topology. For a network of N-coupled PWL-systems, we observe that the node with the smallest scroll-degree governs the collective itinerary of the network, i.e., the dominant node in a ring configuration network is that with smallest scroll-degree. Furthermore, we show that the network can display several behaviors depending on the inner linking matrix Γ. Next, we extend our results to the case in which we remove a link from the network, transforming its topology to a directed chain topology. Here we explore two scenarios: the first node in the chain has the largest scroll-degree, or it has the smallest one. In the first scenario, we observe that all the nodes increase their scroll-degree and ϵ-itinerary synchronization for small ϵ is achieved. For the second scenario we observe that all the nodes reduce scroll-degree and evolve in the same basin of attraction of the master system.

Acknowledgment

E. Campos-Cantón acknowledges CONACYT for the financial support for sabbatical year. M. Nicol thanks the NSF for partial support on NSF-DMS Grant 1600780.

References

[1] Chua, Leon O.; Kocarev, Ljupco; Eckert, Kevin and Itoh, Makoto, *Experimental chaos synchronization in Chua's circuit*, International Journal of Bifurcation and Chaos, 2 (3), 705–708, (1992)

[2] Kennedy, Michael Peter, *Three steps to chaos. II. A Chua's circuit primer*, IEEE Transactions on Circuits and Systems I: Fundamental Theory and Applications, 40 (10) 657–674, (1993)

[3] Liu, Xinzhi; Shen, Xuemin and Zhang, Hongtao, *Multi-scroll chaotic and hyperchaotic attractors generated from Chen system*, International Journal of Bifurcation and Chaos, 22 (2) 1250033, (2012)

[4] Yalçin, Müştak E.; Suykens, Johan A. K.; Vandewalle, Joos and Özoğuz, Serdar, *Families of scroll grid attractors*, International Journal of Bifurcation and Chaos, 12 (1) 23–41, (2002)

[5] Lü, Jinhu and Chen, Guanrong, *Generating multiscroll chaotic attractors: theories, methods and applications*, International Journal of Bifurcation and Chaos, 16 (4) 775–858 (2006)

[6] Campos-Cantón E., *Chaotic attractors based on unstable dissipative systems via third-order differential equation*, Int. J. Mod. Phys. C, 27 (1), 1650008 (2016)

[7] Gámez-Guzmán, L.; Cruz-Hernández, C.; López-Gutiérrez, R. M. and García-Guerrero, E. E., *Synchronization of Chua's circuits with multi-scroll attractors: Application to communication*, Communications in Nonlinear Science and Numerical Simulation, 14 (6) 2765–2775, (2009)

[8] Muñoz-Pacheco, Jesús M.; Zambrano-Serrano, E.: Félix-Beltrán, O.; Gómez-Pavón, L.C.; Luis-Ramos A.; *Synchronization of PWL function-based 2D and 3D multi-scroll chaotic systems,* Nonlinear Dynamics, 70 (2) 1633–1643, (2012)

[9] Boccaletti, Stefano; Latora, V.; Moreno, Y.; Chavez, M. and Hwang, D. U., *Complex networks: Structure and dynamics*, Physics Reports, 424 (4-5) 175–308, (2006)

[10] Min, Fuhong, Luo, Albert C.J. *Periodic and chaotic synchronizations of two distinct dynamical systems under sinusoidal constraints* Chaos, Solitons & Fractals, 45, 998–1011 (2012).

[11] Min, Fuhong, Luo, Albert C.J. *Complex Dynamics of Projective Synchronization of Chua Circuits with Different Scrolls* Int. J. of Bifurc. and Chaos, 25 (05), 1530016 (2015).

[12] Jiménez-López, E.; González-Salas, J. S.; Ontañón-García, L. .; Campos-Cantón, E. and Pisarchik, A. N., *Generalized multistable structure via chaotic synchronization and preservation of scrolls*, Journal of the Franklin Institute, 350 (10) 2853–2866, (2013)

[13] Sun, Jie; Bollt, Erik M. and Nishikawa, Takashi, *Master stability functions for coupled nearly identical dynamical systems*, EPL Europhysics Letters, 85 (6) 60011, (2009)

[14] Zhao, Jun; Hill, David J. and Liu, Tao, *Stability of dynamical networks with non-identical nodes: A multiple V-Lyapunov function method*, Automatica, 47 (12) 2615–2625, (2011)

[15] Ontañón-García, L. J.; Jiménez-López, E.; Campos-Cantón, E. and Basin, M, *A family of hyperchaotic multi-scroll attractors in R^n*, Applied Mathematics and Computation, 233, 522–533, (2014)

[16] Pikovsky, A.; Rosemblum, M.; Kurths, J. (2001). Synchronization: A Universal Concept in Nonlinear Sciences. Cambridge University Press. ISBN 0-521-53352-X.

[17] Rulkov, N.F.; Sushchik, M.M.; Tsimring, L.S. and Abarbanel, H.D.I.; *Generalized synchronization of chaos in directionally coupled chaotic systems,* Phys. Rev. E, 51 (2) 980–994 (1995)

[18] Jun, Ma; Fan, Li; Long, Huang and Wu-Yin, Jin; *Complete synchronization, phase synchronization and parameters estimation in a realistic chaotic system*, Communications in Nonlinear Science and Numerical Simulation, 16 (9) 3770–3785 (2011)

[19] Campos-Cantón, Eric; Femat, R; Barajas-Ramírez, Juan Gonzalo and Campos-Cantón, Isaac, *A multivibrator circuit based on chaos generation*, International Journal of Bifurcation and Chaos, 22 (1) 1250011, (2012)

[20] Wang, Xiao Fan and Chen, Guanrong, *Complex networks: Small-world, scale-free and beyond*, IEEE Circuits and Systems Magazine, 3 (1) 6–20, (2003)